

Advances in anisotropy and formability

Dorel Banabic · Frédéric Barlat · Oana Cazacu ·
Toshihiko Kuwabara

Received: 11 April 2010 / Accepted: 3 June 2010 / Published online: 28 June 2010
© Springer-Verlag France 2010

Abstract This paper presents synthetically the most recent models for description of the anisotropic plastic behavior. The first section gives an overview of the classical models. Further, the discussion is focused on the anisotropic formulations developed on the basis of the theories of linear transformations and tensor representations, respectively. Those models are applied to different types of materials: body centered, faced centered and hexagonal-close packed metals. A brief review of the experimental methods used for characterizing and modeling the anisotropic plastic behavior of metallic sheets and tubes under biaxial loading is presented together with the models and methods developed for predicting and establishing the limit

strains. The capabilities of some commercial programs specially designed for the computation of forming limit curves (FLC) are also analyzed.

Keywords Anisotropy · Yield criteria · Strain rate potentials · Biaxial tensile tests · Forming limit diagrams

Introduction

Given the current trends of globalization and active competition on the world market, especially for automotive one, the reduction of the lead time can be decisive. Virtual manufacturing using finite element analyses may contribute to this reduction. Finite element analysis has been applied extensively to compare design options, understand the influence of process conditions on both formability and structural performance and to reduce the trial and error in the development of tools for optimum performance. Key in improving the accuracy of these analyses is the use of appropriate constitutive and formability models.

Anisotropic plastic stress potentials

Aspects of the constitutive models for metal forming applications were discussed by Barlat [42, 45]. A number of reviews concerning plastic yielding in metals can be found in the literature [14, 41, 311, 317, 318] and this section is only a brief summary from the author's perspective.

Classical anisotropic yield functions

The most popular isotropic yield conditions, verified for many metals, were proposed by Tresca and von Mises

D. Banabic (✉)
CERTETA—Research Centre on Sheet Metal Forming
Technology, Technical University of Cluj Napoca,
Cluj Napoca 400020, Romania
e-mail: banabic@tcm.utcluj.ro

F. Barlat
Materials Mechanics Laboratory, GIFT,
Pohang University of Science and Technology,
San 31 Hyoja-dong, Nam-gu,
Pohang, Gyeongbuk 790-784, Republic of Korea
e-mail: f.barlat@postech.ac.kr

O. Cazacu
Department of Mechanical and Aerospace Engineering,
University of Florida/REEF,
Shalimar, FL 32579, USA
e-mail: cazacu@reef.ufl.edu

T. Kuwabara
Institute of Symbiotic Science and Technology,
Tokyo University of Agriculture and Technology,
2-24-16, Nakacho,
Koganei-shi, Tokyo 184-8588, Japan
e-mail: kuwabara@cc.tuat.ac.jp

and may be expressed in terms of the principal values of the stress (σ_i) or the deviatoric stress (S_i) tensors as [117]

$$\begin{aligned} \phi &= |\sigma_1 - \sigma_2|^a + |\sigma_2 - \sigma_3|^a + |\sigma_3 - \sigma_1|^a \\ &= |S_1 - S_2|^a + |S_2 - S_3|^a + |S_3 - S_1|^a = 2\bar{\sigma}^a \end{aligned} \tag{1}$$

where $\bar{\sigma}$ defines the effective stress. For an exponent $a=2$ or $a=4$, Eq. (1) reduces to von Mises, whereas for $a=1$ and in the limiting case $a \rightarrow \infty$, it leads to Tresca yield condition. Its main advantage is that it provides a good approximation of yield loci computed using the Bishop-Hill crystal plasticity model by setting $a=6$ for BCC and $a=8$ for FCC materials, respectively (see [117, 200]).

For isotropic materials, yield criteria have the same form in any reference frame. For anisotropic materials, yielding properties are directional, thus the expression of the yield criterion depends on the reference frame. The simplest form of the yield criterion is with respect to a coordinate system associated with the axes of symmetry of the material. For instance, due to the symmetry of their thermo-mechanical processing history, sheet metals exhibit orthotropic symmetry characterized by three mutually orthogonal planes of symmetry. These are denoted \mathbf{x} , \mathbf{y} and \mathbf{z} and correspond to the rolling, transverse and normal directions of the sheet, respectively. Hill [118] proposed an extension of the isotropic Mises criterion to orthotropic materials

$$\begin{aligned} \phi &= F(\sigma_{yy} - \sigma_{zz})^2 + G(\sigma_{zz} - \sigma_{xx})^2 + H(\sigma_{xx} - \sigma_{yy})^2 \\ &+ 2(L\sigma_{yz}^2 + M\sigma_{zx}^2 + N\sigma_{xy}^2) = \bar{\sigma}^2 \end{aligned} \tag{2}$$

In this equation, F , G , H , L , M and N are material constants. The validity of this yield function has been explored in numerous experiments, the consensus being that it is well suited to specific metals and textures, especially steel [122, 214]. Hill [120] proposed a non-quadratic yield criterion to describe materials other than steel and derived four special cases from the general form. The general expression of Hill’s [120] criterion accounts for planar anisotropy, provided that the directions of the principal stresses are superimposed with the anisotropy axes. The most widely used expression of this yield criterion is the so-called “Special Case IV,” which applies to materials exhibiting planar isotropy (with an average Lankford coefficient \bar{r}) for plane stress states

$$\phi = |\sigma_1 + \sigma_2|^a + (1 + 2\bar{r})|\sigma_1 - \sigma_2|^a = 2(1 + \bar{r})\bar{\sigma}^a \tag{3}$$

Hill proposed other non-quadratic plane stress yield criteria [122, 123]. Independently from Hill, Hosford [137] used Hershey’s isotropic criterion [117], given by Eq. 1, to describe crystal plasticity results and proposed the follow-

ing generalization [138] for materials exhibiting orthotropic symmetry

$$\phi = F|\sigma_{yy} - \sigma_{zz}|^a + G|\sigma_{zz} - \sigma_{xx}|^a + H|\sigma_{xx} - \sigma_{yy}|^a = \bar{\sigma}^a \tag{4}$$

An important drawback of this as well as of Hill’s [120] criteria is that they do not involve shear stresses. Thus, these criteria cannot account for the continuous variation of plastic properties between the sheet’s \mathbf{x} and \mathbf{y} axes. Barlat and Lian [35] successfully extended Hosford’s [138] criterion to capture the influence of the shear stress

$$\phi = \bar{c}|k_1 + k_2|^a + \bar{c}|k_1 - k_2|^a + (2 - \bar{c})|2k_2|^a = 2\bar{\sigma}^a \tag{5}$$

where \bar{a} , \bar{c} , \bar{h} , and \bar{p} are material coefficients and

$$k_1 = \frac{\sigma_{xx} + \bar{h}\sigma_{yy}}{2}, \quad k_2 = \sqrt{\left(\frac{\sigma_{xx} - \bar{h}\sigma_{yy}}{2}\right)^2 + \bar{p}^2\sigma_{xy}^2} \tag{6}$$

Barlat et al. [36] proposed a yield criterion for a general stress state, denoted Yld91, which extends the isotropic Hershey’s criterion, Eq. 1, to orthotropic symmetry as well. Anisotropy is introduced by replacing the principal values of the stress tensor by those of a stress tensor modified with weighting coefficients. Karafillis and Boyce [159] proposed the following generalization of Hershey’s criterion,

$$\begin{aligned} \phi &= (1 - c)(|S_1 - S_2|^a + |S_2 - S_3|^a + |S_3 - S_1|^a) \\ &+ \frac{3^a c}{2^{a-1} + 1} (|S_1|^a + |S_2|^a + |S_3|^a) = 2\bar{\sigma}^a \end{aligned} \tag{7}$$

where c is a constant, and extended it to orthotropic materials, thus generalizing Yld91.

General methods to describe anisotropy: linear transformations and tensor representations

For pressure independent plasticity, the procedure used by Barlat et al. [36] and Karafillis and Boyce [159] to introduce anisotropy is equivalent with the application of a fourth order linear transformation operator on the stress tensor i.e. $\tilde{\sigma} = \mathbf{L}\sigma$ or on the stress deviator $\tilde{\mathbf{s}} = \tilde{\mathbf{L}}\mathbf{s}$. Thus, an anisotropic yield function is obtained from an isotropic function by substituting the principal value of the stress tensor (or deviator) by the principal value of $\tilde{\sigma}$ or $\tilde{\mathbf{s}}$. The coefficients characterizing anisotropy are the components of the fourth order tensor \mathbf{L} or $\tilde{\mathbf{L}}$. Similar to the stiffness or compliance tensor in elastic anisotropy, the symmetry of a material is reflected by the symmetry of the tensor \mathbf{L} or $\tilde{\mathbf{L}}$. The advantage of this theory is that if the isotropic yield function is convex in the principal stresses space, a property that is relatively easy to check in this space, then the anisotropic extension is automatically convex. This proper-

ty ensures stability in numerical simulations where the anisotropic potential is used.

Some authors realized that the approaches that describe anisotropic behavior proposed thus far did not contain enough coefficients to provide a good description of plastic anisotropy, even in the case of uniaxial tension (e.g., Barlat et al. [38, 39]; Plunkett et al. [233]). Therefore, two or multiple (n) linear transformations were proposed in order to increase the number of anisotropy coefficients, e.g., for $n=2$ and pressure independent plasticity

$$\tilde{\mathbf{s}}' = \mathbf{C}'s, \tilde{\mathbf{s}}'' = \mathbf{C}''s \tag{8}$$

where \mathbf{C}'' and \mathbf{C}' are the two tensors containing the anisotropy coefficients (see Barlat et al. [46]). Examples of such yield functions are given in the next section.

An alternate approach to extend any isotropic yield criterion such as to describe any type of material symmetry was proposed by Cazacu and Barlat [71, 72]. Within the framework of the theory of representation of tensor functions, they developed generalizations of the stress deviator invariants J_2 and J_3 . These generalized invariants were required (a) to be homogeneous functions of degree two and three in stresses, respectively, (b) to reduce to J_2 and J_3 for isotropic conditions, (c) to be insensitive to pressure, and (d) to be invariant to any transformation belonging to the symmetry group of the material. The anisotropic yield criterion is obtained by substituting in the expression of the isotropic criterion the invariants of the stress deviator by their respective anisotropic generalizations. Example of such anisotropic yield functions are given in the next section.

Advanced anisotropic yield criteria for body and faced centered metals

These advanced anisotropic yield criteria include more coefficients and are able to describe with accuracy the anisotropy of the tensile properties (both in yield stresses and Lankford coefficients). BCC and FCC materials deform plastically by dislocation glide on certain slip planes and directions. Because glide can occur indifferently in a direction or its reverse, tension and compression flow stresses are identical at the same amount of deformation. Therefore, the yield function must exhibit inversion symmetry, i.e. $\phi(\sigma_{ij}) = \phi(-\sigma_{ij})$. Moreover, the associated isotropic function must be a good approximation of the crystal plasticity response for an aggregate containing a random distribution of grain orientations.

For plane stress, the anisotropic Yld2000-2d yield function ϕ was defined as [40]

$$\phi = \left| \tilde{S}'_1 - \tilde{S}'_2 \right|^a + \left| 2\tilde{S}''_2 + \tilde{S}''_1 \right|^a + \left| 2\tilde{S}''_1 + \tilde{S}''_2 \right|^a = 2\bar{\sigma}^a \tag{9}$$

In the above equation, $\tilde{S}'_1, \tilde{S}'_2$ and $\tilde{S}''_1, \tilde{S}''_2$ are the principal values of $\tilde{\mathbf{s}}'$ and $\tilde{\mathbf{s}}''$, respectively. It can be shown that eight independent coefficients are available in Yld2000-2d, i.e., three C'_{ij} and five C''_{kl} .

Independently, Banabic and collaborators, based on the Barlat criterion [35], developed since 2000 (see for example [13]) the so-called BBC family criteria [18, 22]. The last version, BBC2005 criterion, was defined as

$$\alpha|\Gamma + \Psi|^a + \alpha|\Gamma - \Psi|^a + (1 - \alpha)|2\Lambda|^a = \bar{\sigma}^a$$

where Γ, Ψ and Λ are expressions of the three plane stress components and anisotropy coefficients. It was shown that this yield function contains eight independent coefficients and that, in fact, it was the same as Yld2000-2d only written in a different form (see [46]).

For a pressure-independent material under a general stress state, Bron and Besson [57] extended Karafillis and Boyce [159] yield function by considering two linear transformations thus obtaining a formulation containing 12 anisotropy coefficients. Under the same general stress state conditions, Barlat et al. [44] proposed the yield function Yld2004-18p, which extends Eq. (9)

$$\phi(s_{\alpha\beta}) = \Phi\left(\tilde{S}'_i, \tilde{S}''_j\right) = \sum_{i,j}^{1,3} \left| \tilde{S}'_i - \tilde{S}''_j \right|^a = 4\bar{\sigma}^a \tag{10}$$

The two transformed stress deviators $\tilde{\mathbf{s}}'$ and $\tilde{\mathbf{s}}''$ can be written in a matrix form as

$$\tilde{\mathbf{s}} \equiv \begin{bmatrix} \tilde{s}_{xx} \\ \tilde{s}_{yy} \\ \tilde{s}_{zz} \\ \tilde{s}_{yz} \\ \tilde{s}_{zx} \\ \tilde{s}_{xy} \end{bmatrix} = \begin{bmatrix} 0 & -c_{12} & -c_{13} & 0 & 0 & 0 \\ -c_{21} & 0 & -c_{23} & 0 & 0 & 0 \\ -c_{31} & -c_{32} & 0 & 0 & 0 & 0 \\ 0 & 0 & 0 & c_{44} & 0 & 0 \\ 0 & 0 & 0 & 0 & c_{55} & 0 \\ 0 & 0 & 0 & 0 & 0 & c_{66} \end{bmatrix} \begin{bmatrix} s_{xx} \\ s_{yy} \\ s_{zz} \\ s_{yz} \\ s_{zx} \\ s_{xy} \end{bmatrix}$$

with the appropriate symbols (prime and double prime) for each transformation, i.e., C'_{ij} for $\tilde{\mathbf{s}}'$ and C''_{ij} for $\tilde{\mathbf{s}}''$. Note that, in this formulation, c_{ij} is different from c_{ji} . Thus, 18 parameters (nine per linear transformation) are available to characterize anisotropy.

As explained above, using the generalized invariants, any isotropic yield criterion can be extended to describe anisotropic materials. In Cazacu and Barlat [71], this approach was used to extend Drucker’s isotropic yield criterion [86], which provides a yield surface that is intermediate between the von Mises and Tresca bounds. The proposed orthotropic criterion [71] is

$$\phi = (J_2^o)^3 - c(J_3^o)^2 = k^2 \tag{11}$$

where J_2^o and J_3^o are the orthotropic generalizations of the principal stress tensor invariants. For full 3-D stress

conditions, the orthotropic criterion (11) involves 18 anisotropy coefficients.

Anisotropic yield criteria for hexagonal-close packed metals

Metals with hexagonal close packed (HCP) crystal structure deform plastically by slip and twinning. As opposed to slip, twinning is a directional shear mechanism: shear in one direction can produce twinning while shear in the opposite direction cannot. For example, in magnesium alloys sheets twinning is not active in tension along any direction in the plane of the sheet, but is easily activated in compression. As a result, the average in-plane compressive yield stress is about half the average in-plane tensile yield stress (e.g. see Lou et al. [201]). Thus, the yield surfaces are not symmetric with respect to the stress free condition (SD effect). Since hcp metal sheets exhibit strong basal textures (*c*-axis oriented predominantly perpendicular to the thickness direction), a pronounced anisotropy in yielding is observed. To account for both strength differential (SD) effects and the anisotropy displayed by HCP metals, Hosford [136] proposed the following modification of Hill's orthotropic yield criterion [118]:

$$A\sigma_{xx} + B\sigma_{yy} - (A + B)\sigma_{zz} + F(\sigma_{yy} - \sigma_{zz})^2 + G(\sigma_{zz} - \sigma_{xx})^2 + H(\sigma_{xx} - \sigma_{yy})^2 = 1. \quad (12)$$

where A, B, F, G, H are material coefficients and $\mathbf{x}, \mathbf{y}, \mathbf{z}$ are normal to the mutually orthogonal planes of symmetry of the material. Since the criterion does not involve shear stresses, it cannot account for the continuous variation of the plastic properties between the material axes of symmetry. Liu et al. [199] have proposed an extension of Hill [118] yield criterion in the form which involves shear terms but, as in Eq. 12, SD effects are due to pressure (first invariant of stress) and not to shear mechanisms.

The rigorous methods proposed to account for initial plastic anisotropy or to describe an average material response over a certain deformation range (see section [General methods to describe anisotropy: linear transformations and tensor representations](#)) can also be used for modeling anisotropy in hexagonal materials. The major difficulty encountered in formulating analytic expressions for the yield functions of HCP metals is related to the description of the tension-compression asymmetry associated to twinning. Recently, yield functions in the three-dimensional stress space that describe both the tension-compression asymmetry and the anisotropic behavior of HCP metals have been developed. To describe yielding asymmetry that results either from twinning or from non-Schmid effects at single crystal

level, Cazacu and Barlat [73] have proposed an isotropic criterion expressed in terms of all invariants of the stress deviator.

$$f \equiv (J_2)^{\frac{3}{2}} - cJ_3 = \tau_Y^3, \quad (13)$$

where τ_Y is the yield stress in pure shear and c is a material constant expressible solely in terms of the uniaxial yield stresses in tension and compression, respectively. For equal yield stresses in tension and compression $c=0$, hence the proposed criterion reduces to the von Mises yield criterion. It was shown that this isotropic yield criterion describes with great accuracy the crystal plasticity simulation results of Hosford and Allen [140] and of Vitek et al [286] for randomly oriented polycrystals (for more details, see Cazacu and Barlat [75]).

The isotropic criterion (13) was further extended such as to incorporate anisotropy using the generalized invariants approach i.e. in the expression of the isotropic yield criterion (13) the invariants of the stress deviator were replaced with the generalized invariants J_2^o and J_3^o , respectively. Comparison between this orthotropic criterion and data on magnesium and its alloys (see Graff et al. [108]) and titanium alloys (see Cazacu and Barlat [73]) show that this anisotropic model accurately describes both anisotropy and tension-compression asymmetry in yielding of these materials. Note that for general stress states (3D conditions), the orthotropic extension of the criterion (13): $f \equiv (J_2^o)^{\frac{3}{2}} - cJ_3^o$ involves 18 anisotropy coefficients. These coefficients can be determined based on Lankford coefficients measured in tension and compression along at least 3 orientations in the plane of the sheet, uniaxial tensile and compressive flow stresses along the same orientations and in the normal direction. However, for hexagonal materials data on *r*-values anisotropy in either tension or compression is generally scarce. The mechanical data that is reported consist mainly of uniaxial and compression flow stresses in the rolling, transverse, and normal directions, respectively. If data is limited for a given material, it is recommended to use the recently developed orthotropic criterion by Nixon et al [226]. This criterion is an extension of the isotropic yield function (13) obtained using one linear transformation on the Cauchy stress tensor $\tilde{\sigma} = \mathbf{L}\sigma$. As an example, Fig. 1 shows comparison between theoretical yield surfaces according to this criterion and experimental data corresponding to fixed values of equivalent plastic strain. Note that for strains below 10%, the predicted yield loci have an elliptical type shape, which is typical for slip dominated plastic deformation. Beyond this strain level, the model predicts that the yield loci have a “triangular shape” and that the tension-compression asymmetry is very pronounced. It is worth noting that this change in

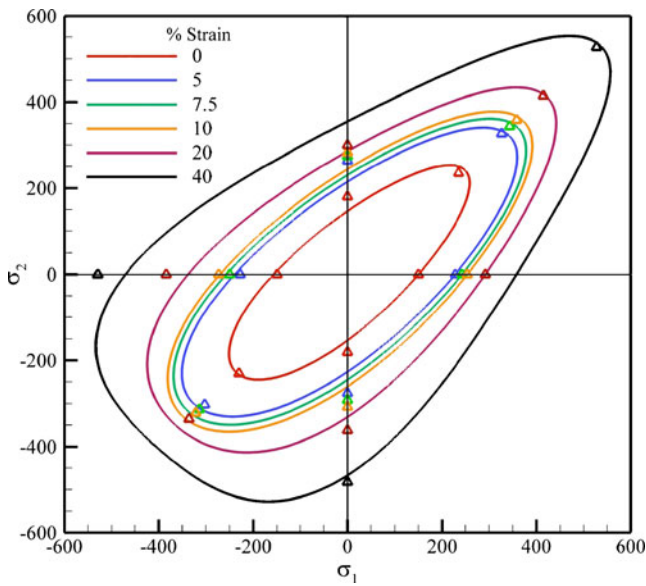


Fig. 1 Theoretical yield surfaces according to Nixon et al. [226] criterion in comparison to experimental data on high purity alpha titanium corresponding to fixed levels of accumulated plastic strain (after Nixon et al. [226]). Principal stresses σ_1 and σ_2 are in MPa

shape occurs at the experimentally determined strain level associated with twin activation in the rolling direction (see Nixon et al., [226]).

Cazacu et al [74] developed another isotropic pressure-insensitive yield criterion that accounts for yielding asymmetry between tension and compression associated with deformation twinning. This isotropic criterion involves all principal values of the stress deviator and is defined as

$$\phi = ||S_1| - kS_1|^a + ||S_2| - kS_2|^a + ||S_3| - kS_3|^a \tag{14}$$

where k is a strength differential parameter while a is the degree of homogeneity. Note that for $k=0$ and $a=2$, this criterion reduces to the von Mises yield criterion. To capture simultaneously anisotropy and tension/compression asymmetry, this isotropic yield criterion was extended to orthotropy by applying a fourth-order linear operator C on the stress deviator s . The anisotropic yield criterion (denoted CPB06) is of the form:

$$F = (|\Sigma_1| - k\Sigma_1)^a + (|\Sigma_2| - k\Sigma_2)^a + (|\Sigma_3| - k\Sigma_3)^a \tag{15}$$

with $\Sigma_1, \Sigma_2, \Sigma_3$ the principal values of the transformed stress tensor $\Sigma = Cs$. Thus, for full 3-D stress states, 9 anisotropy coefficients are involved in the criterion. The orthotropic yield criterion of Eq. 15 was shown to exhibit accuracy in describing the yield loci of magnesium [74] and titanium alloys [74, 163]. Additional linear transformations can be incorporated into the isotropic criterion (14) for an improved representation of the anisotropy (see Plunkett et al. [233] and Fig. 2).

Strain rate potentials

In classical flow theory of plasticity, the yield function serves as a potential for the plastic strain rates (increments), i.e.,

$$\dot{\epsilon}_{ij}^p = \dot{\lambda} \partial \phi / \partial \sigma_{ij} \tag{16}$$

where σ is the Cauchy stress tensor, $\dot{\epsilon}^p$ denotes the plastic strain rate tensor, and $\dot{\lambda} \geq 0$ stands for the plastic multiplier. The yield surface is defined as $\phi(\sigma) = \sigma_T$, where σ_T is the uniaxial yield stress in tension. Using the plastic work equivalence principle, Ziegler [316] proved that a strain rate potential Ψ can be associated to any convex stress potential ϕ . This potential is defined (see [121, 316]) as

$$\psi(\dot{\epsilon}^p) = \dot{\lambda} \tag{17}$$

and the stress is given by the gradient of this potential

$$\sigma = \sigma_T \frac{\partial \psi}{\partial \dot{\epsilon}^p} \tag{18}$$

Hence, a strain rate potential can be also used instead of the classical stress potential to describe the plastic response of the material. Note that, in crystal plasticity, it is easier to numerically obtain the strain rate potential than to compute the yield surface. Further, the crystallographic strain rate potential can be approximated with analytic expressions. Such an approach was applied to single crystals (e.g. Fortunier [97]) and polycrystals with cubic crystal structure (e.g. Arminjon et al. [7]; Van Bael and Van Houtte [274]; Rabahallah et al. [237], etc.). These strain rate potentials have also been used in finite element simulations of forming operations for both FCC and BCC polycrystals (e.g. Yoon et al. [302] etc.). It is worth noting that analytic expressions of the exact strain rate potentials associated to macroscopic stress potentials are known only for classical yield criteria such as von Mises, Tresca, Drucker-Prager, and the anisotropic Hill [118]. For non-quadratic stress potentials, obtaining an analytic expression for the exact dual is very challenging, if not impossible. However, it is possible to develop strain rate potentials that describe the material anisotropy as an independent definition of the material behavior. This is formally identical to developing phenomenological yield functions. Barlat and co-workers have proposed several analytic non-quadratic orthotropic strain rate potentials (see [37, 40, 165]). The strain rate potential proposed by Barlat and Chung [37] has a structure similar to the stress potential Yld91 but in strain rate space. Recently, Barlat and Chung [43] and Kim et al. [165] developed a strain rate potential, called Srp2004-18p,

$$\psi = |\tilde{E}'_1|^b + |\tilde{E}'_2|^b + |\tilde{E}'_3|^b + |\tilde{E}''_2 + \tilde{E}''_3|^b + |\tilde{E}''_3 + \tilde{E}''_1|^b + |\tilde{E}''_1 + \tilde{E}''_2|^b = (2^{2-b} + 2) \dot{\epsilon}^b \tag{19}$$

where $\dot{\bar{\epsilon}}$ is the corresponding effective plastic strain rate and b is an exponent recommended to be 3/2 for BCC and 4/3 for FCC materials, respectively. \tilde{E}'_i and \tilde{E}'' are the principal values of two tensors $\tilde{\epsilon}'$ and $\tilde{\epsilon}''$ resulting from two linear transformations of the strain rate tensor $\dot{\epsilon}$

$$\tilde{\epsilon}' = B'T\dot{\epsilon}, \quad \tilde{\epsilon}'' = B''T\dot{\epsilon}$$

The two 4th order tensors B' and B'' contain the anisotropy coefficients while the 4th order tensor T is necessary to ensure that the gradient of the strain rate potential is deviatoric (T is the 4th order symmetric deviatoric unit tensor, see Kim et al. [165]). Although this strain rate potential is not strictly dual (conjugate) of the respective non-quadratic stress potential Yld 2004-18p, it was shown that it leads to a description of the plastic anisotropy of FCC metals of comparable accuracy to that obtained by the stress potential (see Fig. 3 after Rabahallah et al. [237]).

In general, strain rate potentials are more suitable for process design, especially for the optimization of the initial blank shape for the purpose of reducing the earing

percentage in cup drawing (see Chung et al. [81]). Strain rate potentials are useful for rigid plasticity finite elements (FE) analysis and design codes. Very recently, numerical algorithms for elastic/plastic finite element simulations using this strain-rate potential have been developed (Kim et al [165]; Rabahallah et al. [237]). Stress and strain rate potentials can be used with equal degree of success (e.g., Li et al. [196]) for simulation of forming processes but stress potentials have received more attention in the literature. In summary, the strain rate potentials presented so far (either phenomenological or texture-based) are applicable only to the description of the plastic behavior of materials with cubic crystal structure (BCC or FCC).

Very recently, Cazacu et al [76] have developed an anisotropic strain rate potential applicable to HCP metals. This strain rate potential is the exact dual of the quadratic form of the anisotropic CPB06 stress potential (Eq. (15) with $a=2$). The approach used for deriving this strain-rate potential consisted in first developing an exact dual for the isotropic form of the CPB06 potential. The exact dual of the isotropic form of the CPB06 potential (Eq. (14) with $a=2$) is:

$$\psi = \begin{cases} \frac{1}{m(1-k)} \cdot \sqrt{\dot{\epsilon}_1^2 + \dot{\epsilon}_2^2 + \left[\frac{3k^2 - 10k + 3}{3k^2 + 2k + 3} \right] \dot{\epsilon}_3^2}, & \text{if } \frac{\dot{\epsilon}_3}{\sqrt{\dot{\epsilon}_1^2 + \dot{\epsilon}_2^2 + \dot{\epsilon}_3^2}} \leq \frac{-(3k^2 + 2k + 3)}{\sqrt{6(k^2 + 3)(3k^2 + 1)}} \\ \frac{1}{m(1+k)} \cdot \sqrt{\dot{\epsilon}_1^2 + \dot{\epsilon}_2^2 + \left[\frac{3k^2 + 10k + 3}{3k^2 - 2k + 3} \right] \dot{\epsilon}_3^2}, & \text{if } \frac{\dot{\epsilon}_3}{\sqrt{\dot{\epsilon}_1^2 + \dot{\epsilon}_2^2 + \dot{\epsilon}_3^2}} \geq \frac{3k^2 - 2k + 3}{\sqrt{6(k^2 + 3)(3k^2 + 1)}} \\ \frac{1}{m(1-k)} \cdot \sqrt{\dot{\epsilon}_2^2 + \dot{\epsilon}_3^2 + \left[\frac{3k^2 - 10k + 3}{3k^2 + 2k + 3} \right] \dot{\epsilon}_1^2}, & \text{if } \frac{\dot{\epsilon}_1}{\sqrt{\dot{\epsilon}_1^2 + \dot{\epsilon}_2^2 + \dot{\epsilon}_3^2}} \leq \frac{-(3k^2 + 2k + 3)}{\sqrt{6(k^2 + 3)(3k^2 + 1)}} \\ \frac{1}{m(1+k)} \cdot \sqrt{\dot{\epsilon}_2^2 + \dot{\epsilon}_3^2 + \left[\frac{3k^2 + 10k + 3}{3k^2 - 2k + 3} \right] \dot{\epsilon}_1^2}, & \text{if } \frac{\dot{\epsilon}_1}{\sqrt{\dot{\epsilon}_1^2 + \dot{\epsilon}_2^2 + \dot{\epsilon}_3^2}} \geq \frac{3k^2 - 2k + 3}{\sqrt{6(k^2 + 3)(3k^2 + 1)}} \\ \frac{1}{m(1-k)} \cdot \sqrt{\dot{\epsilon}_3^2 + \dot{\epsilon}_1^2 + \left[\frac{3k^2 - 10k + 3}{3k^2 + 2k + 3} \right] \dot{\epsilon}_2^2}, & \text{if } \frac{\dot{\epsilon}_2}{\sqrt{\dot{\epsilon}_1^2 + \dot{\epsilon}_2^2 + \dot{\epsilon}_3^2}} \leq \frac{-(3k^2 + 2k + 3)}{\sqrt{6(k^2 + 3)(3k^2 + 1)}} \\ \frac{1}{m(1+k)} \cdot \sqrt{\dot{\epsilon}_3^2 + \dot{\epsilon}_1^2 + \left[\frac{3k^2 + 10k + 3}{3k^2 - 2k + 3} \right] \dot{\epsilon}_2^2}, & \text{if } \frac{\dot{\epsilon}_2}{\sqrt{\dot{\epsilon}_1^2 + \dot{\epsilon}_2^2 + \dot{\epsilon}_3^2}} \geq \frac{3k^2 - 2k + 3}{\sqrt{6(k^2 + 3)(3k^2 + 1)}} \end{cases} \quad (20)$$

with $m = \sqrt{\frac{9}{2(3k^2 - 2k + 3)}}$. Note that if there is no difference between the response in tension and compression $k=0$, then the proposed isotropic strain rate potential (20) reduces to $\psi = \sqrt{\frac{2}{3}(\dot{\epsilon}_1^2 + \dot{\epsilon}_2^2 + \dot{\epsilon}_3^2)}$, which is the dual of the von Mises stress potential (i.e. the equivalent plastic strain). As an example, in Fig. 4 is shown the representation in the

octahedral plane of the developed strain rate potential (Eq. 20) for $k=-0.4$ ($\sigma_T/\sigma_C = 0.79$) and $k=0.4$ ($\sigma_T/\sigma_C = 1.26$) along with the von Mises effective strain rate ($k=0$ or $\sigma_T/\sigma_C = 1$), respectively. Note a clear difference in shape between the strain-rate potential (Eq. 20) and the dual of the von Mises strain rate potential (circle). This strong difference is a result

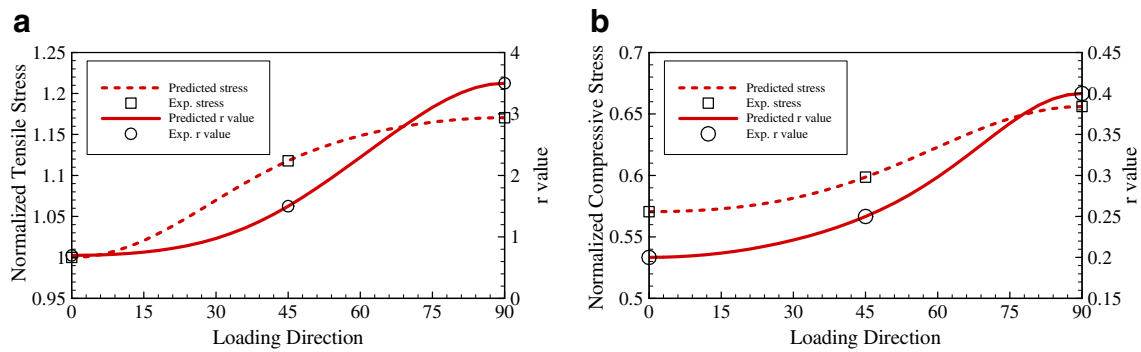


Fig. 2 Anisotropy of the yield stress (normalized by the tensile stress in the rolling direction) and the r-values for AZ31B Mg, measured and predicted with the extension of the yield criterion (14) involving 2

linear transformations for **a** tensile loading; **b** compressive loading (after Plunkett et al. [233]). Experimental data after Lou et al. [201]

of the tension-compression asymmetry of the plastic flow.

It was rigorously proved that the anisotropic extension of this strain rate potential can be obtained by simply substituting in the expression (20) the plastic strain rate tensor $\dot{\epsilon}$ by the modified strain rate tensor $\mathbf{B} = \mathbf{H}:\dot{\epsilon}$, where \mathbf{H} is a fourth-order orthotropic tensor and the constant m by the constant \bar{m} given by:

$$\bar{m} = \left[\frac{1}{(|\Phi_1| - k\Phi_1)^2 + (|\Phi_2| - k\Phi_2)^2 + (|\Phi_3| - k\Phi_3)^2} \right]^{\frac{1}{2}} \quad (21)$$

where $\Phi_1 = \frac{2}{3}C_{11} - \frac{1}{3}C_{12} - \frac{1}{3}C_{13}$; $\Phi_2 = \frac{2}{3}C_{12} - \frac{1}{3}C_{22} - \frac{1}{3}C_{23}$; $\Phi_3 = \frac{2}{3}C_{13} - \frac{1}{3}C_{23} - \frac{1}{3}C_{33}$ and C_{ij} are the components of

the 4th order plastic anisotropy tensor \mathbf{C} involved in the expression of the stress potential CPB06 (see Eq. 15). Furthermore, the tensor \mathbf{H} is the inverse of the tensor $\mathbf{L} = \mathbf{C}\mathbf{T}$, where \mathbf{T} is the 4th order symmetric deviatoric unit tensor. Since the anisotropic strain rate potential $\psi(B, \bar{m})$, with Ψ given by (Eq. 20) and \bar{m} given by (Eq. 21) is an exact dual of the CPB06 stress potential, the anisotropy coefficients are the same as for the stress potential. Thus, the anisotropy coefficients can be determined using either the stress-based formulation or the strain-based formulation in conjunction with mechanical data. Note that for isotropic materials, for which \mathbf{C} reduces to the fourth-order symmetric unit tensor, the anisotropic strain rate potential $\psi(B, \bar{m})$ reduces to the isotropic strain rate potential (Eq. 20). If the material does not display tension-compression asymmetry (yield in tension is equal to the yield in compression), the parameter k associated with strength differential effects is automatically zero and the anisotropic strain rate potential reduces to Hill's [121] orthotropic strain rate potential.

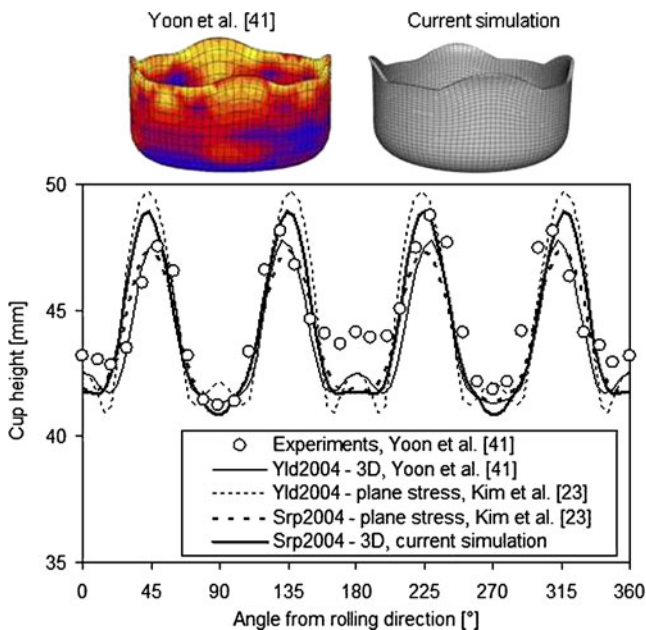


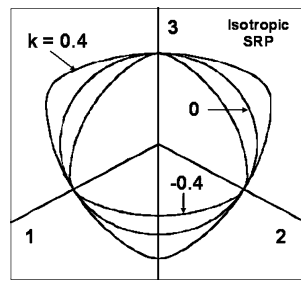
Fig. 3 Finite-element simulations of earing cup profiles for aluminum alloy AA 2090-T3 using the Yld 2004-18p stress potential and Srp2004-18p strain rate potential in comparison with data (after Rabahallah et al. [237])

Discussion

In the past, until the late 1980's yield functions were generic for anisotropic materials. Therefore, they were seldom accurate enough. They did not contain enough anisotropy coefficients and could not describe the anisotropies of the Lankford coefficient and yield stress in uniaxial tension simultaneously. The inversion symmetry was always assumed. To the exception of Hill's [118], the yield functions were applicable to restricted stress cases, for instance formulated with normal stress components only, in order to avoid a number of formulation issues [139]. Therefore, they were not suitable for implementation in finite element codes.

At present, yield functions (or strain rate potentials) are developed for specific materials, FCC, BCC or HCP, and take into account the distinctive features of the response of

Fig. 4 Representation in the octahedral π plane of the isotropic strain rate potential (Eq. 20) corresponding to $k=-0.4, 0.4; k=0$ (Mises effective strain rate), respectively



these materials. For instance, for HCP materials, the inversion symmetry is not imposed anymore. Because of the higher number of anisotropy coefficients, they are more accurate than the yield functions used in the past. In particular, they are able to capture the anisotropy of uniaxial properties (Lankford coefficients and yield stress) simultaneously. The formulations are developed for either plane stress or general stress states without restrictions and can be implemented in finite element codes with relative ease (e.g., Yoon et al. [303–305]; Plunkett et al. [235]). Some efforts are now initiated to formulate macroscopic level models that account for the evolution of anisotropy due to evolving texture. Such macroscopic models were proposed for hexagonal metals by Plunkett et al [232, 235], Nixon et al. [226]. To model the change in shape of the yield locus due to twinning reorientation of the lattice, evolution laws for the anisotropic coefficients involved in the expression of the respective yield function were developed using a multi-scale procedure based on crystal plasticity calculations of flow stresses with the self-consistent viscoplastic model (VPSC) model [190] and macroscopic scale interpolation techniques. Experimental crystallographic textures and stress-strain curves were used as input. This approach was successfully applied to the description of the behavior of zirconium and titanium at room temperature when subjected to quasi-static deformation [226, 232] or dynamic loading [233–235].

In the future, the evolution of yield function coefficients will be self-contained in the formulation for any linear or non-linear loading. Therefore, as in the case of crystal plasticity, it will be possible to describe the evolution of anisotropy as deformation proceeds. However, the computation time will be much lower than what is required for calculations when crystal plasticity models are directly linked to finite element (FE) codes.

Experimental validation of the anisotropic models

In sheet or tube forming processes, materials are generally subjected to multiaxial loads. Therefore, multiaxial loading experiments are highly desirable for validating the plasticity models to be used in simulations. Servo-controlled testing

machines are necessary for such experiments. This section is a brief review of experimental methods for measuring and modeling the anisotropic plastic behavior of metal sheets and tubes under biaxial loading. The reader is also referred to the excellent reviews of earlier work on experimental plasticity by Michno and Findley [217], Hecker [116], Ikegami [147], Bell [48], Phillips [231], Szczepiński [266], Stout and Kocks [257], McDowell [212] and Kuwabara [185].

Hydraulic bulge test

The hydraulic bulging test is widely used in determining the work hardening characteristics of sheet materials up to plastic strains greater than those which can be achieved in simple tension [215]. Several improvements, including a biaxial extensometer [157] and automated hydraulic bulge testers [106, 301] have simplified the experiment somewhat. For an accurate measurement of biaxial stress-strain curves, the geometry of the bulge must be taken into consideration and the strain rate must be constant during bulging [241]. A system for measuring the biaxial yield curve using an optical on-line strain measurement system has been developed [162]. The major limitations of the hydraulic bulging test is the restricted range of stress states, usually from plane strain to balanced biaxial tension, because of the geometry of the die opening, conventionally circular or elliptical.

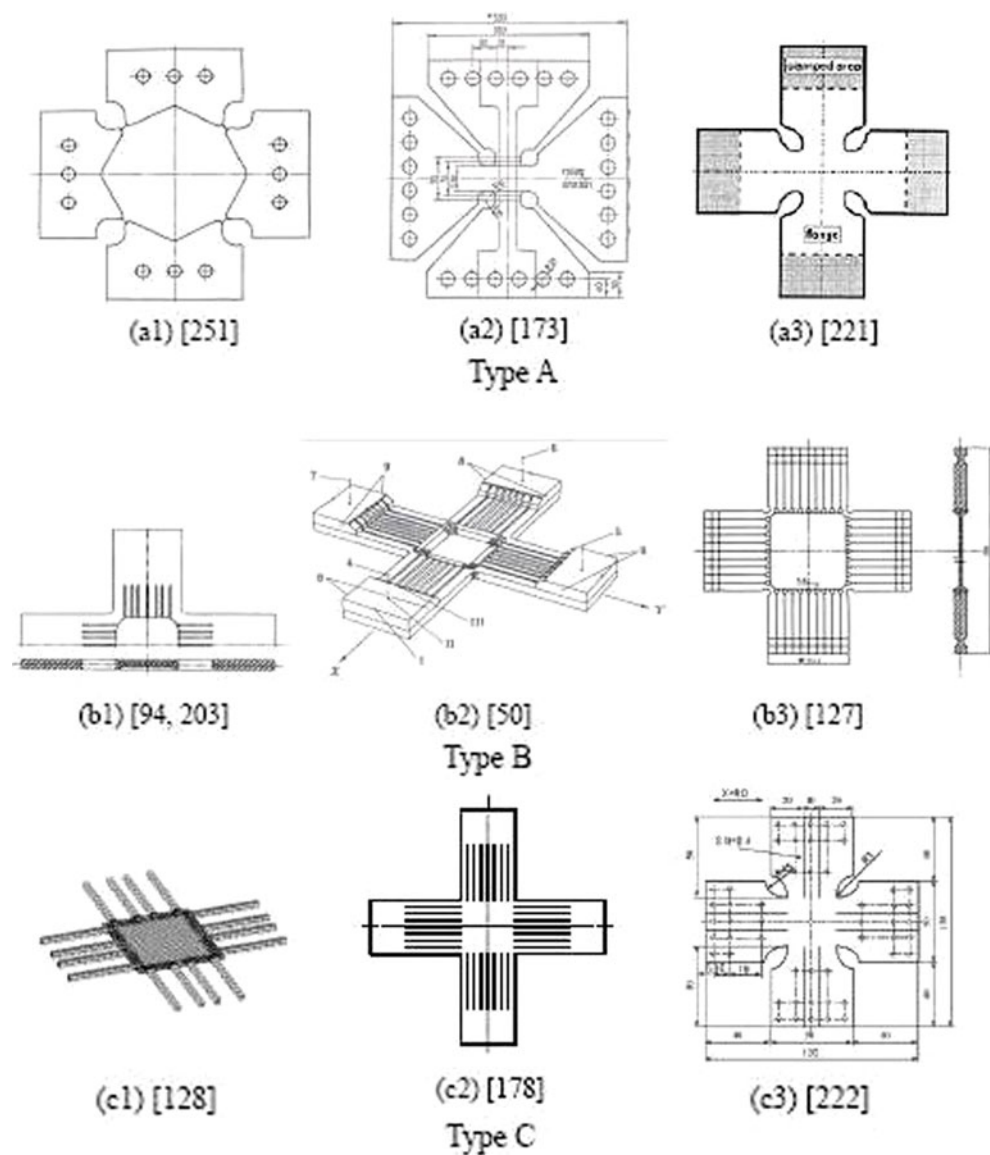
Biaxial compression test

Biaxial compression tests are effective in observing yielding behavior in the π -plane [191, 204, 272]. One of the disadvantages of the biaxial compression test is the difficulty in obtaining accurate stress-strain relations because of friction between the specimen and tool. Moreover, when the plastic deformation mechanism of the material is influenced by the hydrostatic component of stress [202], [256], the yield locus shapes obtained from the biaxial compression experiment may differ from those obtained from the biaxial tension test [202].

Biaxial tension test using a cruciform specimen

Figure 5 shows a variety of cruciform specimens for biaxial tension experiments on metal sheets proposed in the literature. Cruciform specimens are suitable for observing the behavior of sheet metals in small plastic strain ranges of less than several percent. The Type A specimens [173, 221, 251] can be made of as-received sheet materials. However, they do not have slits in the arms; therefore, it is difficult to identifying an effective cross sectional area for determining biaxial stress components accurately. The Type B speci-

Fig. 5 Cruciform specimens for biaxial tension experiments



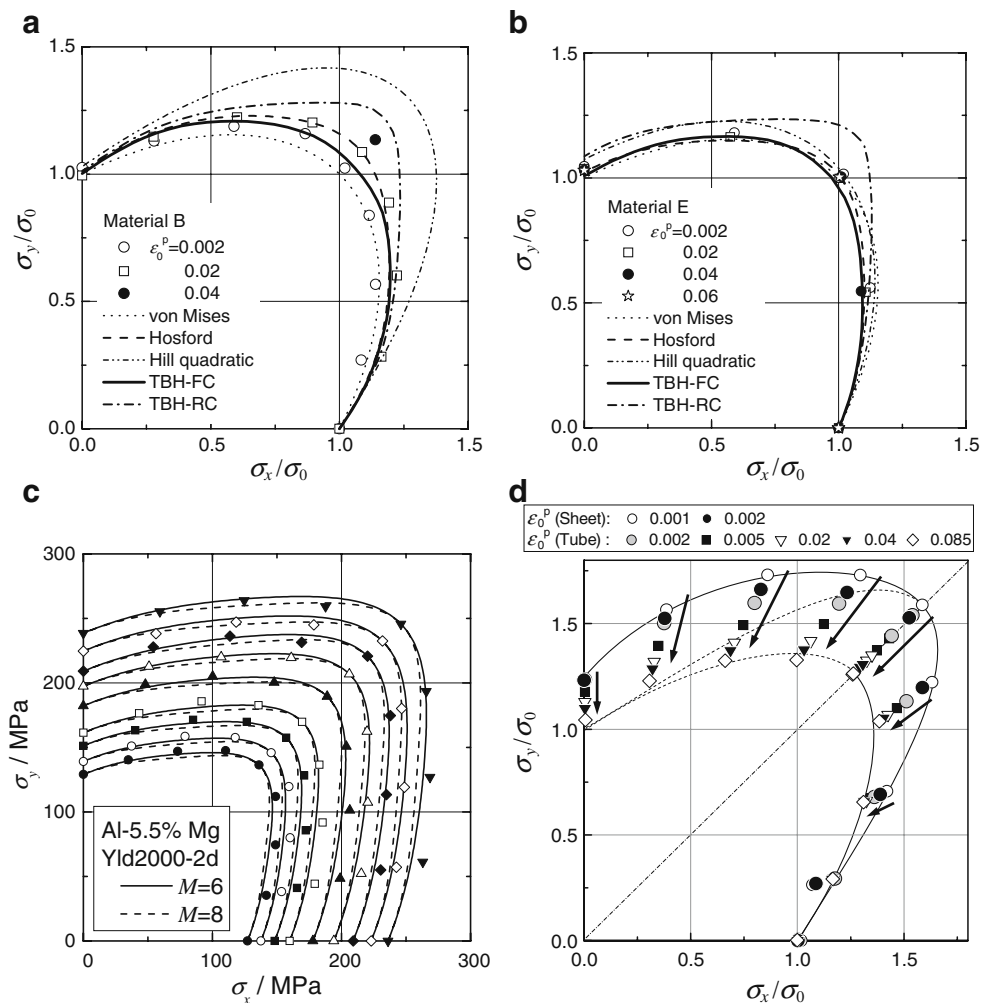
mens [50, 84, 94, 127, 203] have a gauge section thinner than the periphery; therefore, the thick periphery may prohibit uniform deformation of the gauge section. Moreover, it is not easy to create this geometry using as-received metal sheets a few mm thick, common thickness in sheet forming industry. The Type C specimens [52, 128, 178, 222] can be made of as-received sheet materials, although (C1) type specimens [52, 128] require welding for fixing thin strips (arms) to the gauge section. The merit of the Type C specimens is that it is simple to determine biaxial stress components in the gauge section by virtue of slits in the arms or welded thin strips. The number of slits or welded thin strips and its length are important parameters for accurate stress measurement and should be optimized using FEM.

An optimal cruciform specimen geometry for making the stress distribution in the central region uniform and large enough up to fracture was discussed [220, 312].

The reader is also referred to an excellent review of biaxial tensile test devices and cruciform specimen design by Hannon and Tiernan [113].

Figure 6 shows examples of the work contours of sheet metals in the stress space measured using cruciform specimen (c2). Also depicted in the figure are the calculated yield loci based on conventional yield functions and the Taylor-Bishop-Hill (TBH) model. The level of plastic work W per unit volume is represented by the corresponding uniaxial plastic strain ϵ_0^p measured for the uniaxial tension test in the rolling direction of the material. In Fig. 6a, b and d a group of stress points (σ_x, σ_y) comprising a contour of plastic work for a specific value of ϵ_0^p are normalized by the uniaxial tensile flow stress σ_0 corresponding to the ϵ_0^p . It is noted that the shape of the work contours for pure titanium (Fig. 6d) significantly change with increasing ϵ_0^p , showing significant differential work hardening.

Fig. 6 Contours of plastic work and the calculated yield loci for **a** ultra low carbon IF steel [181], **b** cold-rolled dual-phase steel [181], **c** 5000 series aluminum alloy with 5.5% Mg content ($\epsilon_0^p = 0.001, 0.0025, 0.005, 0.01, 0.02, 0.03, 0.04, 0.05, 0.06$) [183] and **d** pure titanium [149], TBH-FC and -RC: Taylor-Bishop-Hill (TBH) model with the full and relaxed constraints



Combined tension-compression test

A new testing device for applying in-plane combined tension-compression stresses to a sheet specimen is developed using comb-shaped dies installed into a biaxial testing machine [186]. Figure 7 shows the measured work contours for a 440 MPa steel alloy and theoretical yield loci calculated using the Yld2000-2d yield function [40] with exponent of six. The yield loci and the directions of plastic strain rates calculated using the Yld2000-2d yield function are in good agreement with the measured work contours for all linear stress paths.

Combined tension-simple shear test

A new experimental technique has been developed for the tension-shear testing of sheet metal [219, 280, 283]. One of the merits of this testing method is that one can obtain the stress-strain curves up to large strain range. On the other

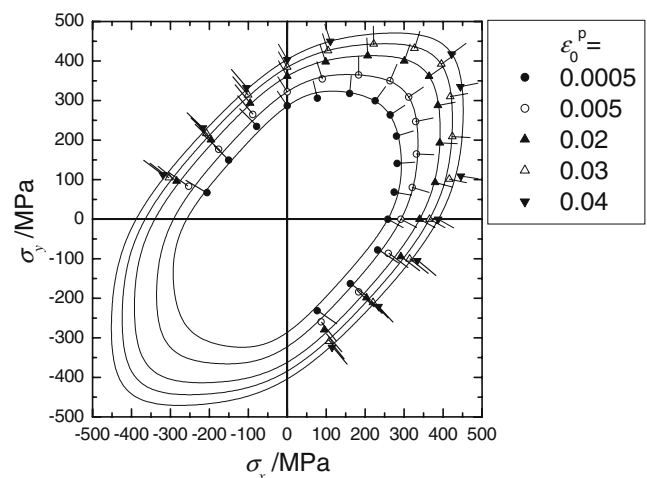


Fig. 7 Comparison of work contours measured for a 440 MPa steel alloy with the Yld2000-2d yield criterion [186]. The short lines attached to the data points represent the directions of the current plastic strain rate

hand, the rotation of the principal axes of stress relative to those of material anisotropy may make it difficult to analyze and formulate the work hardening behavior of the test material.

Biaxial tension test on metal tubes

Multiaxial testing of thin-walled tubular specimens loaded in combined tension-torsion or tension-internal pressure modes is suitable for measuring the behavior of metals subjected to large plastic strain. Anisotropic plastic deformation behavior of brass tube [124], aluminum tube [171, 184], steel tube [310] and pure titanium tube [149] (see Fig. 6d) was observed up to fracture and formulated on the basis of work contours. A yield vertex was successfully observed at the point of loading [179, 182], using the abrupt strain path change method proposed by Kuroda and Tvergaard [174].

Stress reversal test on sheet metals

Stress reversal tests are effective in observing the Baushinger effect of sheet metals: cyclic bending-unbending (Weinmann et al. [292]; Yoshida et al. [306]); cyclic simple shearing (G'sell et al. [110]; Miyauchi [218]; Hu et al. [143]); and in-plane tension/compression stress reversals tests (Iwata et al. [151]; Kuwabara et al. [180, 186, 187]; Yoshida et al. [307], Boger et al. [51], Cao [69]).

Direct stress measurement system

A new experimental approach for determining the local strains and associated stress along multi-axial paths with increasing levels of deformation has been proposed by combining in situ X-ray diffraction (XRD) and a non-contacting commercial 3-D digital image correlation (DIC) [96, 146].

Discussion

In the past, hydraulic bulging tests or biaxial compression tests were widely used. The major limitations are the difficulties in observing accurate stress strain curves in small plastic strain ranges less than several percent and changing stress/strain path during loading.

At present, biaxial tension tests using cruciform specimens are becoming popular for observing the yield locus in the first quadrant of the stress space. If one wishes to observe the anisotropic plastic deformation behavior of sheet metals for large plastic strain ranges up to fracture, one can make thin-walled tubular specimens from a flat sheet and test them using combined tension-torsion or tension-internal pressure testing machines [149, 310].

According to biaxial tension experiments under linear and bilinear stress paths, it has been found that phenomenological plasticity models based on the isotropic hardening assumption, in conjunction with an appropriate anisotropic yield function, are still useful for describing anisotropic plastic deformation behaviors of metal sheets and tubes [185]. If stress reversal plays a dominant role in a forming operation, such as bending-unbending, the Baushinger effect must be measured accurately using a stress reversal test (see [Biaxial tension test on metal tubes](#)) and formulated to make more sophisticated material models.

In the future, material testing based on non-linear loading and multistage loading will be of importance in aid of checking the validity of material models for such loading conditions as those occurring in real forming processes. Measurement and formulation of the non-linear stress-strain relations of prestrained sheet metals subjected to biaxial unloading will be necessary from the viewpoint of improving the accuracy of springback simulations of three dimensional sheet metal parts, such as automotive body panels.

Formability of metallic materials

Formability describes the capability of a sheet metal to undergo plastic deformation in order to get some shape without defects. During the last decades different assessment methods of metals sheets formability have been developed. The most useful tool used to assess formability is the forming limit diagram (FLD). This method meets both manufacturer and user's requirements and is widely used in factory and research laboratories. One of the major advantages of the FLD concept is that the plastic instability can also be described by theoretical models. A detailed presentation of this method can be found in the literature [16, 27, 30, 132, 291, 299].

Prediction of the FLC

Various theoretical models have been developed for the calculation of forming limit curves (FLC).

The first ones were proposed by Swift [265] and Hill [119] assuming homogeneous sheet metals (the so-called models of diffuse necking and localized necking), respectively). The Swift model has been developed later by Hora (so-called Modified Maximum Force Criterion—MMFC) [130, 131]. Marciniak and Kuczynski (MK model) [205] proposed a model taking into account that sheet metals are non-homogeneous from both the geometrical and the microstructural point of view. Stören and Rice [262] have been developed a model based on the bifurcation theory see also ref. [114]). Dudzinski and Molinari [87] used the

method of linear perturbations for analyzing the strain localization and computing the limit strains. Bressan and Williams [56] have introduced so-called “Through Thickness Shear Instability Criterion” in order to take into account the shear fracture mode. Based on the analysis of the influence of the stress distribution through the thickness on the mode of failure, Stoughton [261] has proposed a generalized failure criterion. Since the theoretical models are rather complex and need a profound knowledge of continuum mechanics and mathematics while their results are not always in agreement with experiments, some semi-empirical models have been developed in recent years. The models used for FLC prediction are presented in detail (formulation of the model, solving methods, numerical aspects, advantages and limitations) in [30].

At present, the most widely used models for the computation of the limit strains are those proposed by Marciniak and Kuczynski [205] and Hora [130, 131], respectively. As a consequence, the models previously mentioned will be briefly discussed in the following (see also [16]). The Forming Limit Stress Diagram (FLSD) proposed by Arrieux et al. [8] has been also intensively studied during the last decade.

On the basis of experimental investigations concerning strain localization of specimens subjected to hydraulic bulging or punch stretching, it was concluded that necking is usually initiated by a geometrical or structural non-homogeneity of the material [205]. This non-homogeneity may be associated to a variation of the sheet thickness (geometrical non-homogeneity) or some defects in the microstructure (structural non-homogeneity). The analysis of the necking process have been performed assuming a geometrical non-homogeneity in the form of a thickness variation. This variation is usually due to some defects in the technological procedure used to obtain the sheet metal. The thickness variation is generally gentle. However, the theoretical model assumes a sudden variation in order to simplify the calculations (Fig. 8a). The theoretical model proposed by Marciniak assumes that the specimen has two regions: region “a” having a uniform thickness t_0^a , and region “b” having the thickness t_0^b . The initial geometrical non-homogeneity of the specimen is described by the so-called “coefficient of geometrical non-homogeneity”, f , expressed as the ratio of the thickness in the two regions: $f = t_0^b/t_0^a$. In the MK model, the strain and stress states in the two regions are analyzed and the principal strain ε_1^b in region “b” in relation with the principal strain ε_1^a in region “a” is monitored. When the ratio of these strains $\varepsilon_1^b/\varepsilon_1^a$ becomes too large (infinitely large in theory, but greater than 10 in practice), one may consider that the entire straining of the specimen is localized in region “b”. The shape and position of the curve $\varepsilon_1^a-\varepsilon_1^b$ depend on the value of the f -coefficient. If $f=1$ (geometrically homogeneous

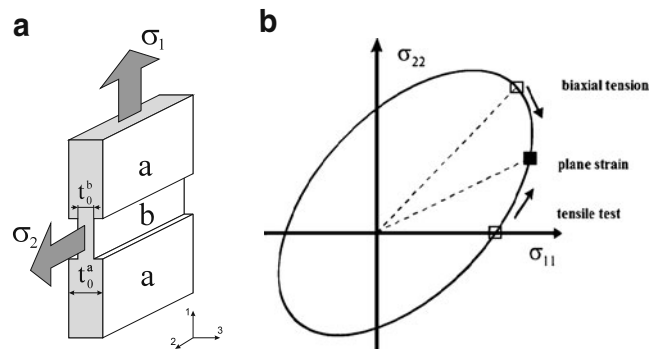
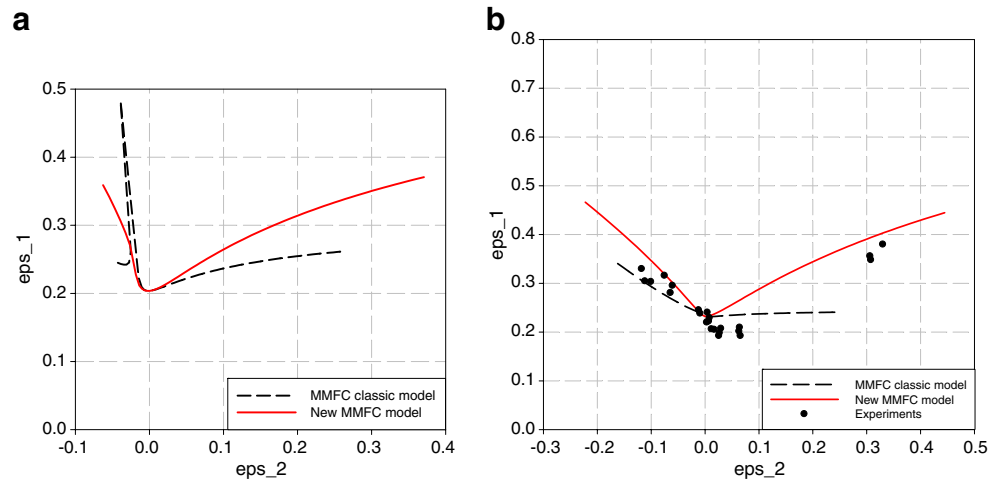


Fig. 8 **a** Geometrical model of the MK theory; **b** basic principle of the MMFC criterion

sheet), the curve becomes coincident with the first bisector. Thus this theory cannot model the strain localization for geometrically homogeneous sheets. The value of the principal strain ε_1^a in region “a” corresponding to non-significant straining of this region as compared to region “b” (the straining being localized in region “b”) represents the limit strain ε_1^{a*} . This strain together with the second principal strain ε_2^{a*} in region “a” define a point belonging to the FLC. Assuming different strain ratios $\rho = d\varepsilon_2/d\varepsilon_1$, one obtains different points on the FLC. Spanning the range $0 < \rho < 1$, one gets the FLC for biaxial tension ($\varepsilon_1 > 0$, $\varepsilon_2 > 0$). In this domain, the orientation of the geometrical non-homogeneity with respect to the principal directions is assumed to be the same during the entire forming process. A detailed analysis of the Marciniak-Kuczynski model (formulation, solving methods, influence on the localization of the deformations etc.) is presented in Chapter 3 of [30].

The ‘Modified Maximum Force Criterion’ (MMFC) for diffuse necking proposed by Hora et al. [130] is based on Considère’s maximum force criterion. The idea behind the MMFC-model is to factor in an additional increase in hardening, which is triggered by the deviation from the initial, homogeneous stress condition—e.g. uniaxial tension—to the stress condition of local necking and with this to the point of plane strain (Fig. 8b) [131]. In order to take into account the influence of the thickness and the strain rate sensitivity index on the limit strains, an enhanced MMFC (eMMFC) has been proposed by Hora et al. [131] and by Brunet [58, 62], respectively. The advantage of the MMFC criteria can be found in their independence of the inhomogeneity assumption. This criterion could be used to calculate FLC for non-linear strain path. A drawback of the MMFC models is the fact that it contains a singularity that emerges if the yield locus contains straight line segments [5, 23, 24, 29] (see the left side of the diagram in the Fig. 9a). To overcome this shortcoming, Comsa and Banabic [82] developed a new

Fig. 9 Prediction of the limit strains using the MMFC classic and new MMFC models for two aluminium alloys: **a** AA2090-T3 and **b** AA5182-T4



version of the MMFC model. Besides eliminating the shortcoming of the MMFC model regarding the possibility of implementing yield loci described by higher order polynomial functions (Fig. 9a), the new model also has the advantage of a better prediction than the classical MMFC model (Fig. 9b).

During the last decade the research in the field of the forming limits prediction have been focused mainly on the following aspects:

Implementation of new constitutive equations in the models used for the computation of the limit strains

The results of the FLC prediction depend crucially on the constitutive equation of the material analyzed. The effect of the shape of the yield locus on the limit strains has been analyzed in detail by Barlat et al. [35]. As we have emphasized in *Anisotropic plastic stress potentials*, a lot of

new yield criteria have been developed during the last decade. Many of those criteria have been already implemented in the computational models of the limit strains, in order to improve the predictive capabilities. Banabic et al. have implemented various yield criteria in the MK model (Hill'93 [12, 17], BBC yield criteria [19, 20, 228] and Cazacu-Barlat [21, 227, 228]. In Fig. 10a is presented the theoretical FLC predicted using BBC2003 criterion versus experimental data for AA5182-0 aluminium alloy [20]. Mattiasson and Sigvant have analyzed in a intensive program the influence of the yield locus shape on necking prediction [208, 210, 211]. Butuc et al. have used the Barlat '97 [64, 66, 67] and BBC2000 [64] yield criteria. Cao [68, 300] used the Karafillis and Boyce [159] yield criterion in the MK model to analyze the effect of changing strain-paths on the FLC. Kuroda and Tvergaard [175] used four different yield criteria to fit a set of experimental data. The Yld 2000 [40] formulation has been included by Aretz

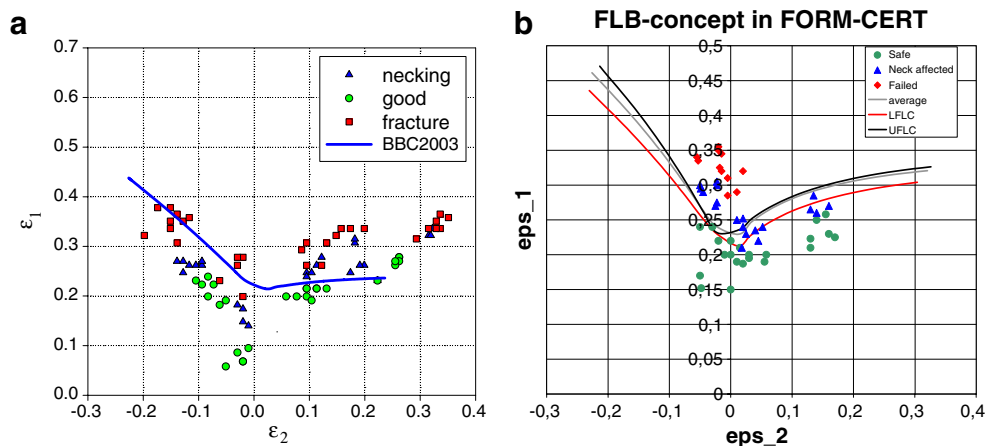


Fig. 10 **a** Theoretical FLC versus experimental data for AA5182-0 aluminium alloy; **b** Predicted Forming Limit Band versus experimental data for AA6111-T43 aluminium alloy (LFLC-lower FLC, UFLC-upper FLC)

[6] in the MK model for studying the influence of the biaxial coefficient of plastic anisotropy on the FLCs. Kim et al. [166] used the Yld2000 [40] criterion to analyze the formability of a sandwich sheets. FLD for multi-layered sandwich sheets considering the material properties of each layer has been formulated with assumption of the visco-rigid plastic material based on the modified MK model [167]. The anisotropic strain-rate potential was utilized for the plastic behavior of each layer. Vegter et al. have implemented their own yield criterion [282–284] in the MK model. Ganjani and Assempour [100–102] have improved the analytical approach for determination of FLC considering the effects of yield functions (Hosford [138], Karafillis-Boyce [159] and BBC2000 [18]). The Teodosiu hardening model [270] associated with different yield criteria has been implemented by Butuc et al. [65] and Haddag et al. [111] in a MK theory for studying the influence of the loading path change on the limit strains. The effect of BBC2003 yield surface on the prediction of FLCs and the number of experimental anisotropy parameters on the accuracy of yield functions are studied by Ahmadi et al. [2]. The polynomial yield function developed by Soare [253] has been implemented in the MK model [254] and has been used to analyze the sensitivity of the MK model to the shape of the yield surface [255].

Implementation of the polycrystalline models

The adaptability of the texture based models to the MK theory of the strain localisation has been proved in the 1980's by Bate [47], Assaro [11], Barlat [33, 34] and later by Van Houtte [275] and Neale [148, 243, 293–295, 297, 315] teams. Later on, Viatkina et al. [285] have used such models for the computation of FLCs. The texture-based yield criterion developed by Van Houtte et al. [276] has been implemented in FLC models, the results being compared both with those provided by phenomenological models and with experimental data [21]. Van Houtte model [276] coupled with a dislocation based hardening model [270] have been implemented by Hiwatashi et al. [126, 278] in order to predict the forming limits corresponding to change strain paths. A microstructural model developed for the description of the aluminium alloy hardening (ALFLOW) has been used by Berstad et al. [49] to predict the forming limits of the AA3103-0 alloy. Boudeau [53, 54] used the linear stability analysis combined with a polycrystalline model to predict and to analyze the influences on the FLC. A polycrystal plasticity model has been used by McGinty [213] to conduct parametric studies of FLC. Knockaert et al. [169] have used a rate-independent polycrystalline plasticity to predict the limit strains. The influence of the texture on the FLCs has been studied by Kuroda [177] and Fjedbo et al. [95]. More recently,

Signorelly et al [247, 248], John Neil and Agnew [156] have analyzed the forming-limit strains using a rate-dependent plasticity, polycrystal, self-consistent (VPSC) model, in conjunction with the Marciniak–Kuczynski (M–K) approach.

Implementation of the ductile damage models

Several types of ductile damage models have been developed during the time, e.g. Gurson, Kachanov, Chaboche, Gologanu (see details in [193]). Those models have been frequently used during the last decade for the computation of the limit strains. Brunet et al. have used the Gologanu model [105] for calculating such limit strains [59–61]. The effects of texture and damage evolution on the limit strains have been studied by Hu et al. [144]. Chow et al. have developed a ductile damage model and implemented it into the MK theory both for linear [78] and complex load paths [79, 80]. An anisotropic model of Gurson type have been used by Huang et al. [145] for the computation of the FLCs. Ragab et al., [240] use a new model to predict the FLC for kinematically hardened voided sheet metals. Han and Kim [112] used an original ductile fracture criterion to calculate the FLC. Lemaitre's ductile damage model has been also implemented by Teixeira [269]. Parsa et al. [229] have determined the Forming Limit Curves for of sandwich sheet using the Gurson damage model.

Enhancing the existing models to take into account new material or process parameters

The influence of different parameters on the limit strains has been analyzed since the end of the 1960's. More recently, several new introduced parameters have been included in the MK and MMFC models: the shape of the yield locus [17], the forming temperature [1, 133, 172, 313] and the coefficient of biaxial anisotropy [6]. The influences of the different effects on the limit strains have been studied: the effect of the surface defects [125], the effect of the void growth [239], the effect of grain size [244], the effect of the curvature and thickness [134]. Brunet and Clerc [62] have extended Hora's model by including the strain rate sensitivity exponent and used it for studying the influence of that parameter on the limit strains. Chan [77] has developed a model of forming limits prediction for the superplastic forming. Predictive models of localized necking for strain-rate-dependent sheet metals have been developed by Mattiasson et al. [209, 210], Zhang et al. [313], Jie et al. [155]. The effect of the normal pressure on the formability of sheet metals is well known and has already been used in industry for a long time [161]. An analysis of sheet failure under normal pressure without

assuming ductile damage has been done in the last period. Such an analysis was performed by using Swift-Hill models by Gotoh [107], Smith [252] and Matin [207]. Recently, Banabic and Soare [28], Wu et al. [298] and Alwood and Shouler [4] have analyzed independently the influence of the normal pressure on the Forming Limit Curve using an enhanced MK model. The experimental researches of the Single Point Incremental Forming (SPIF) [3, 154, 230, 246] showed that the formability of the sheet in this process increases (the FLC is beyond the traditional FLC). Alwood [3] and Jackson [152] have suggested that Through Thickness Shear influences formability in SPIF process. Based on these observations, Eyckens extend the MK model to analyze the influence of the Through Thickness Shear on the FLC [90, 91].

Extending the FLC models for non-linear strain-paths

During the sheet metal forming processes, the material is usually subjected to complex strain patterns. Nakazima [223] has proved that complex loads modify the shape and position of the FLC's. This fact imposes the determination of the limit strains for complex strain-paths. The development of the computational models for complex strain-paths in the frame of the MK theory has become an active research field in the early 1980's (see Barata et al. [31, 32] and also [291]). The refinement of those models has been intensively approached only during the last period. Butuc [63, 65–67] has developed a general computer code for the FLC computation in the case of complex load paths using various hardening models (both phenomenological—Swift, Voce, and microstructural ones—Teodosiu-Hu). Rajarajan et al. [238] have validated the CRACH model for the case of complex strain-paths. Cao [68, 300] analyzed the influence of the changing strain paths on the limit strains. Hiwatashi et al. [126] have used Teodosiu's model for studying the influence on the strain-path change on FLCs. Kuroda and Tvergaard [176] have studied the effect of the strain-path change on the limit strains using four anisotropic models.

Using advanced numerical methods for the solution of the limit strain models

Wagoner and his co-workers have used the finite element method for the numerical determination of the limit strains in the frame of the MK theory [225, 314]. Later on, FEM has been also used by Horstemayer [135], Tai and Lee [267], Nandedkar [224], Gänser et al. [103], Evangelista [89], Van der Boogaard [273], Lademo [188, 189], Berstad [49], Brunet [61], Paraianu [227], Teixeira [269], Hopperstad [129]. The results reported by the researchers previously mentioned are promising.

Modeling the Forming Limit Band concept

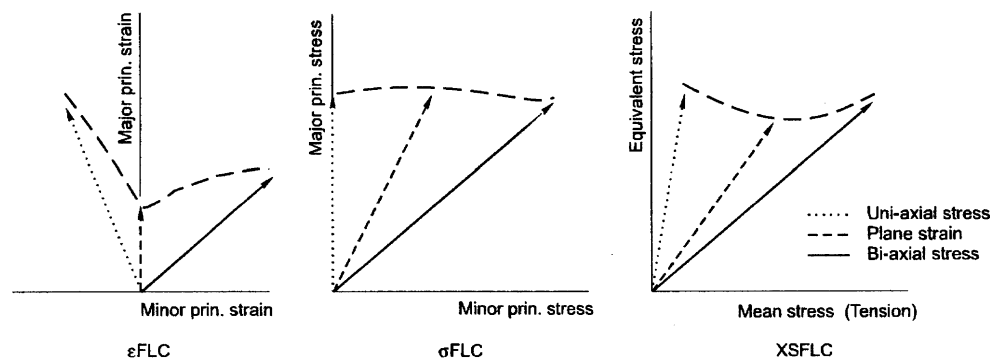
The first results on the influence of the variability of the material parameters on the Forming Limit Curves have been reported by van Minh et al. [279]. Karthik et al. [160] have studied the coil-to-coil, test-to-test and laboratory-to-laboratory variability of sheet formability using OSU formability test. On the basis of the variability of the limit strains established by experiments [70, 242], Janssens et al. [153] introduced the Forming Limit Band concept. This is a strip containing almost all of the limit strain states. The concept has been extended by Strano and Colosimo [263, 264]. Assuming the variability of the mechanical parameters of the sheet metal, Banabic and Vos [26], [290] have developed a computational method of the Forming Limit Band. In the Fig. 10b is presented the predicted Forming Limit Band versus experimental data for AA6111-T43 aluminium alloy. A new model based on the assumption of the thickness variations of the sheet (modeled by use of random fields) to predict the Forming Limit Band has been proposed by Fyllingen et al. [99]. An approach to statistically evaluate the forming limit in hydroforming processes when taking into account the variations in the material parameters has been reported recently by Kim et al. [168].

Forming Limit Stress Diagram (FLSD)

The concept of Forming Limit Stress Diagram (FLSD) proposed by Arrieux et al. [8] has been intensively studied recently. The FLSD is reportedly independent of strain paths [8–10, 109, 259–261, 296, 309]. Biaxial stress experiments on aluminum alloy tube [308] and steel tube [310] for many linear and bilinear stress paths revealed that forming limit stresses are effectively path independent, provided that unloading is included between the loading paths and that the material work hardens isotropically. The FLSD concept therefore appears to be useful, particularly in multistage forming, for predicting the failure of metal tubes and sheets.

In order to extend the application of stress limit curves to a 3-D stress state (presence of through-thickness components of compressive stress), Simha et al. [249] has introduced a new concept, namely Extended Stress-Based Limit Curve (XSFLC). The XSFLC represents the equivalent stress and mean stress at the onset of necking during in-plane loading. Figure 11 shows the three formulations of the Forming Limit Curve concept, namely: strain-based FLC (ϵ FLC), stress-based FLC (σ FLC) and Extended Stress-Based FLC (XSFLC), respectively. Figure 11 also presents the loading paths for the three cases: uniaxial stress, plane strain and biaxial stress. A thorough analysis of the conditions for the use of the XSFLC as a Formability Limit Curve under three-dimensional loading is presented in [250].

Fig. 11 Schematic of the strain-based forming limit curve (ϵ FLC), the stress-based forming limit curve (σ FLC) and the extended stress-based forming limit curve (XSFLC) [250]



Developing commercial codes for FLC computation (see Commercial programs)

Advanced methods to determine the FLC

Since the proposal of the FLC concept, many researchers have been actively involved in the development of experimental methods for the accurate and objective determination of the limit strains. These experimental aspects have been the most important obstacles limiting the practical use of the FLC's. During the last years, the digital processing of the images has allowed the development of refined methods for the experimental measurement of the limit strains. These methods aim to remove the subjective perturbations induced by the human operator in the process of image analysis. More precisely, new algorithms for the detection of the defect occurrence on the formed part have been developed. They have contributed to the increased accuracy of the limit strain measurement and to the reduction of the discrepancy between the experimental data obtained in different laboratories. In the following, we shall present some of these methods. Further details related to this problem can be found in [15, 16, 30, 132].

Takashina and his co-workers [268] first proposed a simple method to determine the limit strains (so-called “three circle method”). The method has been improved by Veerman [281]. Bragard [55] developed in 1972 a more precise

method of determining the limit strains based on interpolation. This method is later improved by D'Haeyer and Bragard [85] using the name of “the double profile method”. In 1972 Hecker [115] proposed a method based on the determination of three types of ellipses around the fracture: fractured, necked and acceptable. The method consists in determining the major and minor strains of the different types of ellipses in the neighborhood of the fracture on the deformed piece and transposing them on FLD. The limit curve is traced between the point corresponding to the ellipses affected by necking and the acceptable ones. The method has been used on a large scale because of simplicity. Kobayashi [170] defines the limit strain based on the accelerated increase of the roughness in the necking area. The Zürich meeting in 1973 of the IDDRG workgroup, following an analysis of several versions of limit strain determination, recommends using an improved version of the Bragard method. This is known as the “Zürich Nr.5 method” [216]. A review of these methods can be found in References [15] and [30].

Together with the development “of online” video strain measuring methods, new methods of determining the limit strains have been proposed in the last years. A new criterion based on the evolution of the strain rate as a function of time during the forming process has been proposed by the SOLLAC team [206]. The method is based on the observation that the beginning of the necking is accompanied by a considerable increase of the strain rate (see Fig. 12a).

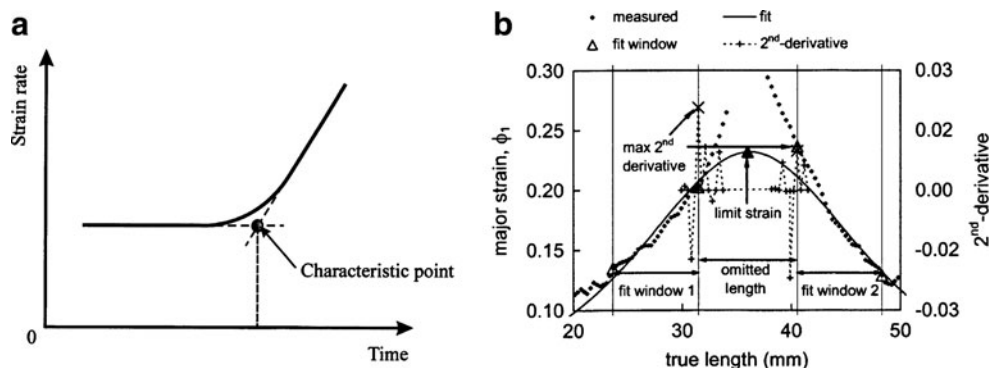


Fig. 12 Methods to determine the limit strains: **a** Strain-rate versus time; **b** IDDRG method

According to this method the start necking point corresponds to the dramatic change in the strain-rate versus time variation (characteristic point). This point could be determined by the intersection of the two straight lines corresponding to the first and the last sector of the curve. The strain—rate evolutions are automatically determined by images analysis. The strain-rate method has been used recently by Volk [287]. He used the idea to identify a regular grid for the optical measurement as a typical mesh of a finite element method. Leppin et al. [194] proposed a method to correct the effect of non-proportional strain paths on Nakajima test based Forming Limit Curves.

The Nakajima workgroup of the IDDRG has developed a new method [141], the so-called “in-process measurement” method (see Fig. 12b). A guideline for the determination of FLC based on this method is presented in the papers [142] and [197]. The method is similar to that of Bragard. Using a video camera system, a film of the forming process is made. Based on the film of the forming process, the development of the strain distribution starting from the onset of necking and finally up to the fracture is analyzed. The method is very robust and leads to a good repeatability of the results. Base of this achievements, the expert group of Nakajima workgroup proposed a revision of the ISO 12004 standard “Metallic materials-sheet and strip-Determination of the forming limit curves” [150]. Recently, the formability of a wide range of materials was assessed using traditional Nakajima FLD testing at different labs and compared with results obtained using the analysis method in the revised ISO/DIS 12004-2 standard, for position dependent testing after fracture [271].

Based on the video camera measurement some systems have been developed by the commercial company to determine automatically the FLC. CAMSYS company has developed the first automatically system (ASAME—Automated Strain Analysis and Measurement Environment) used on the large scale, both in research laboratory and industry [195]. The INSA Lyon developed a FLC determination system (IcaForm) based on the spray of a random pattern of paint at the surface of the sample to determine strain distribution [58]. An opto-mechanical device adaptable allows determining easily the FLC. An objective criterion to identify the start of local necking automatically has been proposed recently [245]. The “Autogrid” system developed by Vialux company offer the possibility to determine the limit strains automatically and independent of any operator. The methodology used to define the limit strain is presented in details in the papers [92] and [93]. GOM Company has developed for the FLC determination so-called ARAMIS system [98]. The methodology used is according with the Nakajima workgroup recommendation [141]. For an FLC, five different geometries are used, for each geometry three specimens and for each specimen three

to five parallel sections. The FLC determination procedure can be done automatically. Eberle [88] has proposed a fully automatic and time-dependent method of determining the beginning of the plastic instability based on physical effects. The regular grid of the optical measurement is treated as a mesh of a finite element calculation. The new method has been used successful for the FLC experimental determinations in the Benchamrk 1 “Virtual Forming Limit Curves” of the NUMISHEET 2008 Conference [288, 289].

Commercial programs

In the last decade, more commercial programs for the limit strains prediction have been developed. In this section the most significant ones are presented.

Based on a Marciniak-Kuczynski model [205], Jurco and Banabic [25, 158] have developed so-called FORM-CERT commercial code. The BBC 2003 yield criterion [22] is implemented in this model. This yield criterion can be reduced to simpler formulations (Hill’48, Hill’79, Barlat’89, etc). In this way, the yield criterion can be also used in the situations when only 2, 4, 5, 6, or 7 mechanical constants are available. The program consists in four modules: a graphical interface for input, a module for the identification and visualization of the yield surfaces, of the strain hardening laws and a module for calculating and visualizing the forming limit curves. The numerical results can be compared with experimental data, using the import/export facilities included in the program. The FORM-CERT code can be directly coupled with the finite element codes.

Hora and his co-workers [132] have developed MAT-FORM code based on the MMFC model. This code is able to calculate and plot the limit strains and also the visualization of the strain hardening curve and yield loci using Hill’48, Hill’79, Hill’90 and Barlat’89 criteria. The program is useful for evaluation of most common experiments like tensile, bulge, Miyauchi, torsion dilatometer and tube hydroforming tests. The program is very well documented and is able to export the constitutive models in FEM specific form for the application in the mostly spread FEM-codes like Autoform or PamStamp.

Using the CRACH algorithm (based on the Marciniak-Kuczynski model), Gese and Dell [104] have developed two software: CrachLAB, a product for prediction of the initial FLC and CrachFEM a product for coupling with the FEM codes. Criteria for ductile and shear fracture have been included in CrachFEM to cover the whole variety of fracture modes for sheet materials. The material model used to calculate instability describes: the initial anisotropy (using Hill’48 and Dell models), the combined isotropic-kinematic hardening and the strain rate sensitivity [83]. CrachFEM is now included in the FEM codes PamStamp and PamCrash of ESI Group.

Discussion

In the past, the FLC models provided an approximate description of the experimental results. Such models were used especially for obtaining qualitative information concerning the necking/tearing phenomena.

At present, the FLC models allow a sufficiently accurate prediction of the limit strains, but each model suffers from its own limitations (see [Prediction of the FLC](#)). There is no model that can be applied to any sort of sheet metal, any type of crystallographic structure, any strain-path or any variation range of the process parameters (strain rate, temperature, pressure, etc.).

The future research will be focused on a more profound analysis of the phenomena accompanying the necking and fracture of the sheet metals. On the basis of the analysis, more realistic models will be developed in order to obtain better predictions of the limit strains. New models will be developed for prediction of the limit strains for special sheet metal forming processes: superplastic forming, forming at very high pressure, incremental forming etc. Commercial codes allowing the quick and accurate calculation of the FLC's both for linear and complex strain-paths will be developed. The texture models will be also implemented in such commercial programs. The FLC computation will be included in the finite element codes used for the simulation of the sheet metal forming processes. The aim is to develop automatic decision tools (based on artificial intelligence methods) useful in the technological design departments. The stochastic modeling of the FLC's will be developed in order to increase the robustness of the sheet metal forming simulation programs. More refined, accurate and objective experimental methods for the experimental determination of the limit strains (e.g. methods based on thermal or acoustic effects) will be also developed.

Acknowledgments The work done by Dorel Banabic was supported by the Romanian National University Research Council in the frame of the project PCCE ID-100.

References

1. Abedrabbo N, Pourboghrat F, Carsley J (2006) Forming of aluminum alloys at elevated temperatures. *Int J Plast* 22:314–373
2. Ahmadi S, Eivani AR, Akbarzadeh A (2009) An experimental and theoretical study on the prediction of Forming Limit Diagrams using new BBC yield criteria and M–K analysis. *Comput Mater Sci* 44:1272–1280
3. Allwood JM, Shouler DR, Tekkaya AE (2007) The increased forming limits of incremental sheet forming processes. *Key Eng Mat* 344:621–628
4. Allwood JM, Shouler DR (2008) Generalised forming limit diagrams showing increased forming limits with non-planar stress states. *Int J Plast* 25:1207–1230
5. Aretz H (2004) Numerical restrictions of the modified maximum force criterion for prediction of forming limits in sheet metal forming. *Model Simulat Mater Sci Eng* 12:677–692
6. Aretz H (2006) Impact of the equibiaxial plastic strain ratio on the FLD prediction. In: Juster N, Rosochowski A (eds.), *Proc. 9th ESAFORM Conference on Material Forming*. Glasgow, April 2006. AKAPIT, Krakow, 311–314
7. Arminjon M, Imbault D, Bacroix B, Raphanel JL (1994) A fourth-order plastic potential for anisotropic metals and its analytical calculation from the texture function. *Acta Mech* 107:33–51
8. Arrieux R, Bedrin C, Boivin M (1982) Determination of an intrinsic Forming Limit Stress Diagram for isotropic sheets. In: *Proc. of the 12th IDDRG Congress*. S-ta Margherita Ligure, 61–71
9. Arrieux R, Bedrin C, Boivin M (1985) Determination of the strain path influence of the forming limit diagrams, from the limit stress curve. *Annals of the CIRP* 34:205–208
10. Arrieux R (1987) Determination of the Forming Limit Stress Curve for Anisotropic Sheets. *Annals of the CIRP* 36:195–198
11. Asaro RJ, Needleman A (1985) Texture development and strain hardening in rate-dependent polycrystals. *Acta Metall* 33:923–953
12. Banabic D (1999) Limit strains in the sheet metals by using the 1993 Hill's yield criterion. *J Mater Process Tech* 92-93:429–432
13. Banabic D, Comsa DS, Balan T (2000) A new yield criterion for orthotropic sheet metals under plane-stress conditions. In: Banabic D (ed) *Proc. of the 7th Conf. TPR2000*. Cluj Napoca, 217–224
14. Banabic D (2000) Anisotropy of Sheet Metals. In: Banabic D (ed) *Formability of metallic materials*. Springer-Verlag, Berlin, pp 119–172
15. Banabic D (2000) Forming Limits of Sheet Metals. In: Banabic D (ed) *Formability of metallic materials*. Springer-Verlag, Berlin, pp 173–215
16. Banabic D (2000) Theoretical models of the FLD's. In: Banabic D (ed) *Formability of metallic materials*. Springer-Verlag, Berlin, pp 317–327
17. Banabic D, Dannenmann E (2001) The influence of the yield locus shape on the limits strains. *J Mater Process Tech* 109:9–12
18. Banabic D, Kuwabara T, Balan T, Comsa DS, Julean D (2003) Non-quadratic yield criterion for orthotropic sheet metals under plane-stress conditions. *Int J Mech Sci* 45:797–811
19. Banabic D et al (2004) FLD theoretical model using a new anisotropic yield criterion. *J Mater Process Tech* 157-158:23–27
20. Banabic D (2004) Anisotropy and formability of AA5182-0 aluminium alloy sheets. *Annales of CIRP* 53:219–222
21. Banabic D, et al. (2004) Prediction of FLC from two anisotropic constitutive models. In: Stören S (ed) *Proc. 7th ESAFORM Conference on Material Forming*. Trondheim, 455–459
22. Banabic D, Aretz H, Comsa DS, Paraianu L (2005) An improved analytical description of orthotropy in metallic sheets. *Int J Plast* 21:493–512
23. Banabic D, Aretz H, Paraianu L, Jurco P (2005) Application of various FLD modelling approaches. *J Model Simulat Mater Sci Eng* 13:759–769
24. Banabic D, Cazacu O, Paraianu L, Jurco P (2005) Recent developments in the formability of aluminum alloys. In: Smith LM, Pourboghrat F, Yoon J-W, Stoughton TB (eds) *Proc. of the NUMISHEET 2005 Conference*. AIP 466–472
25. Banabic D (2006) Numerical prediction of FLC using the M-K-Model combined with advanced material models. In: Hora P (ed) *Numerical and experimental methods in prediction of forming limits in sheet forming and tube hydroforming processes*. ETH Zürich, Zürich, pp 37–42
26. Banabic D, Vos M (2007) Increasing the robustness in the simulation of sheet metal forming processes using a new concept—Forming Limit Band. *Annales of CIRP* 56:249–252

27. Banabic D, Barlat F, Cazacu O, Kuwabara T (2007) Anisotropy and formability. In: Chinesta F, Cueto E (eds) *Advances in material forming-ESAFORM 10 years on*. Springer, Heidelberg-Berlin, pp 143–173
28. Banabic D, Soare S (2008) On the effect of the normal pressure upon the forming limit strains. In: Hora P (ed) *Proc. of the NUMISHEET 2008 Conf., Interlaken, Switzerland*, 199–204
29. Banabic D, Soare S (2009) Assessment of the modified maximum force criterion for aluminum metallic sheets. *Key Eng Mat* 410-411:511–520
30. Banabic D et al (2010) *Sheet metal forming processes*. Springer, Heidelberg
31. Barata da Rocha A, Jalinier JM (1984) Plastic instability of sheet metals under simple and complex strain path. *Trans Iron Steel Inst Jpn* 24:133–140
32. Barata da Rocha A, Barlat F, Jalinier JM (1985) Prediction of the forming limit diagrams of anisotropic sheets in linear and non-linear loading. *Mater Sci Eng* 68:151–164
33. Barlat F, Richmond O (1985) Prediction of tricomponent plane stress yield surfaces and associated flow and failure behavior of strongly textured FCC sheets. *Mater Sci Eng* 95:15–29
34. Barlat F (1987) Crystallographic texture, anisotropic yield surfaces and forming limits of sheet metals. *Mater Sci Eng* 91:55–72
35. Barlat F, Lian J (1989) Plastic Behavior and Stretchability of Sheet Metals. Part I: yield function for orthotropic sheets under plane stress conditions. *Int J Plast* 5:51–66
36. Barlat F, Lege DJ, Brem JC (1991) A six-component yield function for anisotropic materials. *Int J Plast* 7:693–712
37. Barlat F, Chung K (1993) Anisotropic potentials for plastically deforming. *Metals, Model Simul Mater Sci Eng* 1:403–416
38. Barlat F, Becker RC, Hayashida Y, Maeda Y, Yanagawa M, Chung K, Brem JC, Lege DJ, Matsui K, Murtha SJ, Hattori S (1997) Yielding description of solution strengthened aluminum alloys. *Int J Plast* 13:185–401
39. Barlat F, Maeda Y, Chung K, Yanagawa M, Brem JC, Hayashida Y, Lege DJ, Matsui K, Murtha SJ, Hattori S, Becker RC, Makosey S (1997) Yield function development for aluminum alloy sheets. *J Mech Phys Solid* 45:1727–1763
40. Barlat F, Brem JC, Yoon JW, Chung K, Dick RE, Lege DJ, Pourboghrat F, Choi S-H, Chu E (2003) Plane stress yield function for aluminum alloy sheet-Part I: Theory. *Int J Plast* 19:1297–1319
41. Barlat F, Cazacu O, Zyczowski M, Banabic D, Yoon JW (2004) Yield surface plasticity and anisotropy. In: Raabe D, Roters F, Barlat F, Chen L-Q (eds) *Continuum scale simulation of engineering materials—fundamentals—microstructures—process applications*. WileyVCH Verlag, Manheim, pp 145–177
42. Barlat F (2005) Constitutive modeling for metals. In: Banabic D (ed) *Proc. 8th ESAFORM Conference on Material Forming*. Cluj-Napoca April 2005. The Publishing House of the Romanian Academy, Bucharest, 3–10
43. Barlat F, Chung K (2005) Anisotropic strain rate potential for aluminum alloy plasticity. In: Banabic D (ed) *Proc. 8th ESAFORM Conference on Material Forming*. Cluj-Napoca April 2005. The Publishing House of the Romanian Academy, Bucharest, 415–418
44. Barlat F, Aretz H, Yoon JW, Karabin ME, Brem JC, Dick RE (2005) Linear transformation-based anisotropic yield functions. *Int J Plast* 21:1009–1039
45. Barlat F (2007) Constitutive modeling for metals. In: Banabic D (ed) *Advanced methods in material forming*. Springer-Verlag, Berlin, pp 5–25
46. Barlat F, Yoon JW, Cazacu O (2007) On linear transformations of stress tensors for the description of plastic anisotropy. *Int J Plast* 23:876–896
47. Bate P (1984) The prediction of limit strains in steel sheet using a discrete slip plasticity model. *Int J Mech Sci* 26:373–384
48. Bell JF (1984) The Experimental Foundations of Solid Mechanics. In: Truesdell C (ed) *Mechanics of Solids*, vol I. Springer-Verlag, Berlin
49. Berstad T et al. (2004) FEM and a microstructure based work-hardening model used to calculate FLCs. In: Stören S (ed) *Proc. 7th ESAFORM Conference on Material Forming*. Trondheim, 131–134
50. Boehler JP, Demmerle S, Koss S (1984) A new direct biaxial testing machine for anisotropic materials. *Exp Mech* 34:1–9
51. Boger RK, Wagoner RH, Barlat F, Lee MG, Chung K (2005) Continuous, large strain, tension/compression testing of sheet material. *Int J Plast* 21:2319–2343
52. Borsutzki M, Keßler L, Sonne H-M (2002) Kennzeichnung des Verfestigungsverhaltens von Werkstoffen mit der Biaxialprüfung. In: *Werkstoffprüfung 2002, Proc. DVM-Conference*, Bad Nauheim, 186 (in German)
53. Boudeau N, Gelin JC, Salhi S (1998) Computational prediction of the localized necking in sheet forming based on microstructural material aspects. *Comput Mater Sci* 11:45–64
54. Boudeau N, Gelin JC (2000) Necking in sheet metal forming. Influence of macroscopic and microscopic properties of materials. *Int J Mech Sci* 42:2209–2232
55. Bragard A, Baret JC, Bonnarens H (1972) A simplified technique to determine the FLD at onset of necking. *CRM* 33:53–63
56. Bressan JD, Williams JA (1983) The use of a shear instability criterion to predict local necking in sheet metal deformation. *Int J Mech Sci* 25:155–168
57. Bron F, Besson J (2003) A yield function for anisotropic materials. Application to aluminum alloys. *Int J Plast* 20:937–963
58. Brunet M, Morestin F (2001) Experimental and analytical necking studies of anisotropic sheet metals. *J Mater Process Tech* 112:214–226
59. Brunet M, Morestin F, Walter H (2001) Damage modeling in sheet metals forming processes with experimental validations. In: Habraken AM (ed) *Proc. 4th ESAFORM Conference on Material Forming*. Liege, 209–212
60. Brunet M, Morestin F, Walter H (2002) Anisotropic ductile fracture in sheet metal forming processes using damage theory. In: Pietrzyk M, Mitura Z, Kaczmaj J (eds) *Proc. 5th ESAFORM Conference on Material Forming*. Krakow, 135–138
61. Brunet M, Morestin F, Walter-Laberre H (2005) Failure analysis of anisotropic sheet metals using a non-local plastic damage model. *J Mater Process Tech* 170:457–470
62. Brunet M, Clerc P (2007) Two prediction methods for ductile sheet metal failure. In: *Proc. 10th ESAFORM Conference on Material Forming*, Zaragoza, 297–302
63. Butuc C et al (2002) A more general model for FLD prediction. *J Mater Process Tech* 125-126:213–218
64. Butuc C, et al. (2002) Influence of constitutive equations and strain-path change on the forming limit diagram for 5182 Aluminum Alloy. In: Pietrzyk M, Mitura Z, Kaczmaj J (eds) *Proc. 5th ESAFORM Conference on Material Forming*, Krakow, 715–719
65. Butuc C, Gracio JJ, Barata da Rocha A (2003) A theoretical study on forming limit diagrams prediction. *J Mater Process Tech* 142:714–724
66. Butuc C, Gracio JJ, Barata da Rocha A (2005) Application of the YLD 96 yield criterion on describing the anisotropy and formability of the BCC materials. In: Banabic D (ed) *Proc. 8th ESAFORM Conference on Material Forming*. Cluj-Napoca April 2005. The Publishing House of the Romanian Academy, Bucharest, 391–394

67. Butuc C et al (2006) An experimental and theoretical analysis on the application of stress-based forming limit criterion. *Int J Mech Sci* 48:414–429
68. Cao J et al (2000) Prediction of localized thinning in sheet metal using a general anisotropic yield criterion. *Int J Plast* 16:1105–1129
69. Cao V, Lee W, Cheng HS, Seniw M, Wang H-P, Chung K (2009) Experimental and numerical investigation of combined isotropic-kinematic hardening behavior of sheet metals. *Int J Plast* 25:942–972
70. Carleer B, Sigvant M (2006) Process scatter with respect to material scatter. In: Liewald M (ed) *New developments in sheet metal forming*. Institute for Metal Forming Technology, University of Stuttgart, 225–239
71. Cazacu O, Barlat F (2001) Generalization of Drucker's yield criterion to orthotropy. *Math Mech Solid* 6:613–630
72. Cazacu O, Barlat F (2003) Application of representation theory to describe yielding of anisotropic aluminum alloys. *Int J Eng Sci* 41:1367–1385
73. Cazacu O, Barlat F (2004) A criterion for description of anisotropy and yield differential effects in pressure-insensitive metals. *Int J Plast* 20:2027–2045
74. Cazacu O, Plunkett B, Barlat F (2006) Orthotropic yield criterion for hexagonal close packed metals. *Int J Plast* 22:1171–1194
75. Cazacu O, Barlat F (2008) Modeling plastic anisotropy and strength differential effects in metallic materials. In: Cazacu O (ed) *Multiscale modeling of heterogeneous materials: from microstructure to macroscale properties*. ISTE Ltd and John Wiley & Sons, Inc, 71–91
76. Cazacu O, Ionescu IR, Yoon JW (2009) Orthotropic strain rate potential for description of anisotropy in tension and compression of metals. *Int. J. Plast.* <http://dx.doi.org/10.1016/j.ijplas.2009.11.005>
77. Chan KC, Tong GQ (2003) Formability of high-strain-rate superplastic Al-4.4Cu-1.5Mg/21SiCW, composite under biaxial tension. *Mater Sci Eng A* 340:49–57
78. Chow CL et al (1997) A unified damage approach for predicting FLDs. *Trans ASME, J Eng Mater Tech* 119:346–353
79. Chow CL, Yang XJ (2001) Prediction of the FLD on the basis of the damage criterion under non-proportional loading. *Proc Inst Mech Eng* 215C:405–414
80. Chow CL et al (2001) Prediction of FLD for AL6111-T4 under non-proportional loading. *Int J Mech Sci* 43:471–486
81. Chung K, Yoon JW, Richmond O (2000) Ideal sheet forming with frictional constraints. *Int J Plast* 16:595–610
82. Comsa DS, Banabic D (2010) An improved version of the Modified Maximum Force Criterion (MMFC)
83. Dell H, Gese H, Oberhofer G (2008) Advanced yield loci and anisotropic hardening in the material model MF GENYLD + CRACHFEM. In: Hora P (ed) *Proc. of the NUMISHEET 2008 Conf.*, Interlaken, Switzerland, 49–54
84. Demmerle S, Boehler JP (1983) Optimal design of biaxial tensile cruciform specimens. *J Mech Phys Solid* 41:143–181
85. d'Hayer R, Bragard A (1975) Determination of the limiting strains at the onset of necking. *CRM* 42:33–35
86. Drucker DC (1949) Relation of experiments to mathematical theories of plasticity. *J Appl Mech* 16:349–357
87. Dudzinski D, Molinari A (1988) Instability of visco-plastic deformation in biaxial loading. *CR Acad Sci Paris* 307:1315–1321
88. Eberle B, Volk W, Hora P (2008) Experimental FLC with a full 2D approach based on a time depending method. In: Hora P (ed) *Proc. of the NUMISHEET 2008 Conf.*, Interlaken, Switzerland, 279–284
89. Evangelista SH et al (2002) Implementing a modified Marciniak-Kuczynski model using the FEM for the simulation of sheet metal deep drawing. *J Mater Process Tech* 130-131:135–144
90. Eyckens P, Van Bael A, Van Houtte P (2008) An extended Marciniak-Kuczynski forming limit model to assess the influence of Through-Thickness Shear on formability. In: Hora P (ed) *Proc. of the NUMISHEET 2008 Conf.* Interlaken, Switzerland, pp 193–198
91. Eyckens P, Van Bael A, Van Houtte P (2009) Marciniak-Kuczynski type modelling of the effect of Through-Thickness Shear on the forming limits of sheet metal. *Int J Plast* 25, (in press)
92. Feldmann P, Schatz M (2006) Effective evaluation of FLC-tests with the optical in-process strain analysis system AUTOGRID. In: Hora P (ed) *Numerical and experimental methods in prediction of forming limits in sheet forming and tube hydroforming processes*. ETH Zürich, Zürich, pp 69–73
93. Feldmann P (2007) Application of strain analysis system AUTOGRID for evaluation of formability tests and for strain analysis on deformed parts. In: Tisza M (ed) *Proc. of the IDDRG 2007 Conference*, Gyor, 483–490
94. Ferron G, Makinde AJ (1988) Design and development of a biaxial strength testing device. *J Test Eval* 16:253–256
95. Fjeldbo SK, et al. (2005) A numerical study on the onset of plastic instability in extruded materials with strong through-thickness texture variation. In: Banabic D (ed) *Proc. 8th ESAFORM Conference on Material Forming*. Cluj-Napoca April 2005. The Publishing House of the Romanian Academy, Bucharest, 209–213
96. Foecke T, Iadicola MA, Lin A, Banovic SW (2007) A method for direct measurement of multiaxial stress-strain curves in sheet metal. *Metal Mater Trans A* 38A:306–313
97. Fortunier R (1989) Dual potentials and extremum work principles in single crystal plasticity. *J Mech Phys Solid* 37:779–790
98. Friebe H et al (2006) FLC determination and forming analysis by optical measurement system. In: Hora P (ed) *Numerical and experimental methods in prediction of forming limits in sheet forming and tube hydroforming processes*. ETH Zürich, Zürich, pp 74–81
99. Fyllingen O et al (2009) Estimation of forming limit diagrams by the use of the finite element method and Monte Carlo simulation. *Comput Struct* 87:128–139
100. Ganjani M, Assempour A (2007) An improved analytical approach for determination of FLD considering the effects of yield functions. *J Mater Process Tech* 182:598–607
101. Ganjani M, Assempour A (2007) The performance of Karafillis-Boyce yield function on determination of forming limit diagrams. *IJE Transactions A: Basics* 20:55–66
102. Ganjani M, Assempour A (2008) Implementation of a robust algorithm for prediction of forming limit diagrams. *J Mater Eng Perform* 17:1–6
103. Gänser HP, Werner EA, Fisher FD (2000) FLDs: a micro-mechanical approach. *Int J Mech Sci* 42:2041–2054
104. Gese H, Dell H (2006) Numerical prediction of FLC with the program CRACH. In: Hora P (ed) *Numerical and experimental methods in prediction of forming limits in sheet forming and tube hydroforming processes*. ETH Zürich, Zürich, pp 43–49
105. Gologanu M et al (1997) Recent extension of Gurson's model for porous ductile metals. In: Suquet P (ed) *Continuum micromechanics*. Springer-Verlag, Berlin, pp 61–130
106. Gologranc F (1975) Gerät zur kontinuierlichen aufnahme von fließkurven an blechwerkstoffen im hydraulischen tiefungsversuch. *Ind Anz* 97:937–938
107. Gotoh M, Chung T, Iwata N (1995) Effect of out-of-plane stress on the forming limit strains of sheet metals. *JSME Int J* 38:123–132
108. Graff S, Brocks W, Steglich D (2007) Yielding of magnesium: from single crystals to polycrystalline aggregates. *Int J Plast* 23:1957–1978

109. Gronostajski J (1985) Application of limit stresses to determine limit strains at complex strain paths. *Archiwum Hutnictwa* 30:41–56
110. G'sell C, Boni S, Shrivastava S (1983) Application of the plane simple shear test for determination of the plastic behaviour of solid polymers at large strains. *J Mater Sci* 18:903–918
111. Haddag B, Abed-Meraim F, Balan T (2008) Strain localization and damage prediction during sheet metal forming. In: P (ed) Proc. 11th ESAFORM Conference on Material Forming. Lyon
112. Han HN, Kim KH (2003) A ductile fracture criterion in sheet metal forming process. *J Mater Process Tech* 142:231–238
113. Hannon A, Tiernan AP (2008) A review of planar biaxial tensile test. *J Mater Process Tech* 98:1–13
114. Hashiguchi K, Protasov A (2004) Localized necking analysis by the subloading surface model with tangential-strain rate and anisotropy. *Int J Plast* 20:1909–1930
115. Hecker SS (1972) A simple forming limit curve technique and results on aluminum alloys. In: proc. of the IDDRG Congress, Amsterdam, 5.1–5.8
116. Hecker SS (1976) Experimental studies of yield phenomena in biaxially loaded metals. In: Stricklin JA, Saczalski KH (eds) Constitutive equations in viscoplasticity: computational and engineering aspects. ASME, New York, pp 1–33
117. Hershey AV (1954) The plasticity of an isotropic aggregate of anisotropic face centred cubic crystals. *J Appl Mech* 21:241–249
118. Hill R (1948) A theory of the yielding and plastic flow of anisotropic metals. *Proc Roy Soc Lond A* 193:281–297
119. Hill R (1952) On discontinuous plastic states, with special reference to localized necking in thin sheets. *J Mech Phys Sol* 1:19–30
120. Hill R (1979) Theoretical plasticity of textured aggregates. *Math Proc Cambridge Philos Soc* 85:179–191
121. Hill R (1987) Constitutive dual potential in classical plasticity. *J Mech Phys Solid* 35:23–33
122. Hill R (1990) Constitutive modelling of orthotropic plasticity in sheet metals. *J Mech Phys Solid* 38:405–417
123. Hill R (1993) A user-friendly theory of orthotropic plasticity in sheet metals. *Int J Mech Sci* 35:19–25
124. Hill R, Hecker SS, Stout MG (1994) An investigation of plastic flow and differential work hardening in orthotropic brass tubes under fluid pressure and axial load. *Int J Solids Struct* 31:2999–3021
125. Hiroi T, Nishimura H (1997) The influence of surface defects on the forming-limit diagram of sheet metal. *J Mater Process Tech* 72:102–109
126. Hiwatashi S, Van Bael A, Van Houtte P, Teodosiu C (1998) Prediction of the forming limit strains under strain-path changes: application of an anisotropic model based on texture and dislocation structure. *Int J Plast* 14:647–669
127. Hjelm HE (1994) Yield surface for gray cast iron under biaxial stress. *Trans ASME J Eng Mat Tech* 116:148–154
128. Hoferlin E, Van Bael A, Van Houtte P, Steyaert G, De Maré C (2000) The design of a biaxial tensile test and its use for the validation of crystallographic yield loci. *Model Simulat Mater Sci Eng* 8:423–433
129. Hopperstad OS et al. (2006) A preliminary numerical study on the influence of PLC on the formability of aluminium alloys. In: Juster N, Rosochowski A (eds) Proc. 9th ESAFORM Conference on Material Forming. Glasgow, April 2006. AKAPIT, Krakow, 315–318
130. Hora P, Tong L (1994) Prediction methods for ductile sheet metal failure using FE-simulation. In: Proc. of the IDDRG Congress. Lisbon, 363–375
131. Hora P, Tong L, Reissner J (1996) A prediction method for ductile sheet metal failure. In: Lee JK, Kinzel, GL, Wagoner RH (eds) Proc. of the NUMISHEET 1996 Conference, Dearborn, 252–256
132. Hora P, Krauer J (eds) (2006) Numerical and experimental methods in prediction of forming limits in sheet metal forming and tube hydroforming processes. FLC-Zürich 06 Conference, Zürich
133. Hora P, et al. (2007) Numerical and experimental evaluation of thermal dependent FLC. In: Tisza M (ed) Proc. of the IDDRG 2007 Conference, Gyor, 23–30
134. Hora P, Tong L (2008) Theoretical prediction of the influence of curvature and thickness on the FLC by the enhanced modified maximum force criterion. In: Hora, P. (ed.): Proc. of the NUMISHEET 2008 Conf., Interlaken, Switzerland 205–210
135. Horstemeyer MF, Chiesa ML, Bamman DJ (1994) Predicting FLDs with explicit and implicit FE codes. In: Proc. SAE Conference, Detroit, 481–495
136. Hosford WF (1966) Texture strengthening. *Metals Eng Quarterly* 6:13–19
137. Hosford WF (1972) A generalized isotropic yield criterion. *J Appl Mech Trans ASME* 39:607–609
138. Hosford WF (1979) On yield loci of anisotropic cubic metals. In: Proceedings 7th North American Metalworking Conference, SME, Dearborn MI, 191–197
139. Hosford WF (1985) Comments on anisotropic yield criteria. *Int J Mech Sci* 27:423–427
140. Hosford WF, Allen TJ (1973) Twinning and directional slip as a cause for strength differential effect. *Met Trans* 4:1424–1425
141. Hotz W (2006) European efforts in standardization of FLC. In: Hora P (ed) Numerical and experimental methods in prediction of forming limits in sheet forming and tube hydroforming processes. ETH Zürich, Zürich, pp 24–25
142. Hotz W, Timm J (2008) Experimental determination of Forming Limit Curves (FLC). In: Hora P (ed) Proc. of the NUMISHEET 2008 Conf., Interlaken, Switzerland, 271–278
143. Hu Z, Rauch EF, Teodosiu C (1992) Work hardening behavior of mild steel under stress reversal at large strains. *Int J Plast* 8:839–856
144. Hu JG et al (1998) Influence of damage and texture evolution on limit strain in biaxially stretched aluminium alloy sheets. *Mater Sci Eng A* 251:243–250
145. Huang HM, Pan J, Tang SC (2000) Failure prediction in anisotropic sheet metals under forming operations with consideration of rotating principal stretch directions. *Int J Plast* 16:611–633
146. Iadicola M, Foecke T, Ma L (2009) Method for local measurement of stress and strain in a formed part under load. In: Levy BS, Matlock DK, Van Tyne CJ (eds) Proc. Of the IDDRG 2009 Conf., Golden, Colorado, 85–96
147. Ikegami K (1979) Experimental plasticity on the anisotropy of metals. In: Boehler JP (ed) Mechanical behavior of anisotropic solids. Proceedings of the Euromech Colloquium 115, Colloques Inter. du CNRS, Paris, 201–242
148. Inal K, Neale KW, Aboutajeddine A (2005) Forming limit comparisons for FCC and BCC sheets. *Int J Plast* 21:1255–1266
149. Ishiki M, Kuwabara T, Yamaguchi M, Maeda Y, Hayashida Y (2008) Differential work hardening behavior of pure titanium sheet under biaxial loading: In: Hora P (ed) Proc. of the NUMISHEET 2008 Conf., Interlaken, Switzerland, 161–166
150. ISO 12004 (2006) Metallic materials-sheet and strip-Determination of the forming limit curves
151. Iwata N, Matsui M, Kato T, Kaneko K, Tsutsumori H, Suzuki N, Gotoh M (2001) Numerical prediction of spring-back behavior of a stamped metal sheet by considering material nonlinearity during unloading. In: Mori K (ed) Proc. 7th Int. Conf. Numerical Methods in Industrial Forming Processes, Balkema, 693
152. Jackson K, Allwood J (2009) The mechanics of incremental sheet forming. *J Mater Process Tech* 209:1158–1174
153. Janssens K, Lambert F, Vanrostenbergh S, Vermeulen M (2001) Statistical evaluation of the uncertainty of experimentally characterised forming limits of sheet steel. *J Mater Process Tech* 112:174–184

154. Jeswiet J, Young D (2005) Forming limit diagrams for single-point incremental forming of aluminium sheet. *Proc IMechE: J Eng Manufact Part B* 219:1–6
155. Jie M, Cheng CH, Chan LC, Chow CL (2009) Forming limit diagrams of strain-rate-dependent sheet metals. *Int J Mech Sci* 51:269–275
156. John Neil C, Agnew SR (2009) Crystal plasticity-based forming limit prediction for non-cubic metals: Application to Mg alloy AZ31B. *Int J Plast* 25:379–398
157. Johnson W, Duncan JL (1965) The use of the biaxial test extensometer. *Sheet Met Ind* 42:271–275
158. Jurco P, Banabic D (2005) A user-friendly programme for calculating forming limit diagrams. In: Banabic D (ed) *Proc. 8th ESAFORM Conference on Material Forming*. Cluj-Napoca April 2005. The Publishing House of the Romanian Academy, Bucharest, 423–427
159. Karafillis AP, Boyce MC (1993) A general anisotropic yield criterion using bounds and a transformation weighting tensor. *J Mech Phys Solid* 41:1859–1886
160. Karthik V et al (2002) Variability of sheet formability and formability testing. *J Mater Process Tech* 121:350–362
161. Keeler SP (1970) La formabilité est améliorée par pression hydrostatique. *Machine Moderne*, 43–45
162. Keller S, Hotz W, Friebe H, Klein M (2009) Yield curve determination using the bulge test combined with optical measurement. In: Levy BS, Matlock DK, Van Tyne CJ (eds) *Proc. of the IDDRG 2009 Conf.* Golden, Colorado, 319–330.
163. Khan AS, Kazmi R, Farroch B (2007) Multiaxial and non-proportional loading responses, anisotropy and modeling of Ti-6Al-4V titanium alloy over wide ranges of strain rates and temperatures. *Int J Plast* 23:931–950
164. Kim D, Barlat F, Bouvier S, Rabahallah M, Balan T, Chung K (2007) Non-quadratic anisotropic potential based on linear transformation of plastic strain rate. *Int J Plast* 23:1380–1399
165. Kim JH, Lee M-G, Barlat F, Wagoner RH, Chung K (2008) An elasto-plastic constitutive model with plastic strain rate potentials for anisotropic cubic metals. *Int J Plast* 24:2298–2334
166. Kim KJ et al (2003) Formability of AA5182/polypropylene/AA5182 sandwich sheets. *J Mater Process Tech* 139:1–7
167. Kim D, et al. (2008) Formulation of forming limit diagram for sandwich sheet with anisotropic strain-rate potential. In: Hora P (ed) *Proc. of the NUMISHEET 2008 Conf.*, Interlaken, Switzerland, 337–342
168. Kim J, Kang B-S, Lee JK (2009) Statistical evaluation of forming limit in hydroforming process using plastic instability combined with FORM. *Int J Adv Manuf Tech* 42:53–59
169. Knockaert R et al (2000) Forming limits prediction using rate-independent polycrystalline plasticity. *Int J Plast* 16:179–198
170. Kobayashi T, Ishigaki H, Tadayuki A (1972) Effect of strain ratios on the deforming limit of steel sheet and its application to the actual press forming. In: *Proc. of the IDDRG Congress*, Amsterdam, 8.1–8.4
171. Korkolis YP, Kyriakides S (2008) Inflation and burst of anisotropic aluminum tubes for hydroforming applications. *Int J Plast* 24:509–543
172. Krauer J, Hora P, Tong L (2008) Temperature dependent forming limit prediction for metastable stainless steels. In: Hora P (ed) *Proc. of the NUMISHEET 2008 Conf.*, Interlaken, Switzerland, 235–240
173. Kreißig R, Schindler J (1986) Some experimental results on yield condition in plane stress state. *Acta Mech* 65:169–179
174. Kuroda M, Tvergaard V (1999) Use of abrupt strain path change for determining subsequent yield surface: illustrations of basic idea. *Acta Mater* 47:3879–3890
175. Kuroda M, Tvergaard V (2000) FLD for anisotropic metal sheets with different yield criteria. *Int J Solids Struct* 37:5037–5059
176. Kuroda M, Tvergaard V (2000) Effect of strain path change on limits to ductility of anisotropic metal sheets. *Int J Mech Sci* 42:867–887
177. Kuroda M (2005) Effects of texture on mechanical properties of aluminium alloys sheets and texture optimization strategy. In: Smith LM, Pourboghra F, Yoon J-W, Stoughton TB (eds) *Proc. of the NUMISHEET 2005 Conf.* AIP, 445–450
178. Kuwabara T, Ikeda S, Kuroda T (1998) Measurement and analysis of differential work hardening in cold-rolled steel sheet under biaxial tension. *J Mater Process Tech* 80-81:517–523
179. Kuwabara T, Kuroda M, Tvergaard V, Nomura K (2000) Use of abrupt strain path change for determining subsequent yield surface: experimental study with metal sheets. *Acta Mater* 48:2071–2079
180. Kuwabara T, Nagata K, Nakako T (2001) Measurement and analysis of the Bauschinger effect of sheet metals subjected to in-plane stress reversals. In: Torralba JM (ed) *Proc. AMPT '01*, Univ. Carlos III de Madrid, Madrid, 407
181. Kuwabara T, Van Bael A, Iizuka E (2002) Measurement and analysis of yield locus and work hardening characteristics of steel sheets with different R-values. *Acta Mater* 50:3717–3729
182. Kuwabara T, Ishiki M, Kuroda M, Takahashi S (2003) Yield locus and work-hardening behavior of a thin-walled steel tube subjected to combined tension-internal pressure. *Journal de Physique IV* 105:347–354
183. Kuwabara T, Umemura M, Yoshida K, Kuroda M, Hirano S (2005) Forming limits of 5000 series aluminum alloys with different magnesium contents. In: Banabic D (ed) *Proc. 8th ESAFORM Conference on Material Forming*. Cluj-Napoca April 2005. The Publishing House of the Romanian Academy, Bucharest, 399–402
184. Kuwabara T, Yoshida K, Narihara K, Takahashi S (2005) Anisotropic plastic deformation of extruded aluminum alloy tube under axial forces and internal pressure. *Int J Plast* 21:101–117
185. Kuwabara T (2007) Advances in experiments on metal sheets and tubes in support of constitutive modeling and forming simulations. *Int J Plast* 23:385–419
186. Kuwabara T, Horiuchi Y, Uema N, Ziegelheimova J (2008) Material testing method of applying in-plane combined tension-compression stresses to sheet specimen. In: Asnafi (ed) *Proc. of the IDDRG 2008 Conf.* Olofstrom, Sweden, 163–171
187. Kuwabara T, Kumano Y, Ziegelheim J, Kurosaki I (2009) Tension-compression asymmetry of phosphor bronze for electronic parts and its effect on bending behavior. *Int J Plast* 25:1759–1776
188. Lademo OG, Berstad T, Hopperstad OS, Pedersen KO (2004) A numerical tool for formability analysis of aluminium alloys. *Steel Grips 2* (2004) Suppl. *Metal Forming 2004*, Krakow, 427–437
189. Lademo OG et al (2005) Prediction of plastic instability in extruded aluminium alloys using shell analysis and a coupled model of elasto-plasticity and damage. *J Mater Process Tech* 166:247–255
190. Lebensohn RA, Tomé CN (1993) A selfconsistent approach for the simulation of plastic deformation and texture development of polycrystals: application to Zirconium alloys. *Acta Metallurgica et Materialia* 41:2611–2624
191. Lee D, Backofen WA (1966) An experimental determination of the yield locus for titanium and titanium-alloy sheet. *Trans TMS-AIME* 236:1077–1084
192. Lee WB, Tai WH, Tang CY (1997) Damage evolution and forming limit predictions of an AA2024-T3 aluminium alloy. *J Mater Process Tech* 63:100–104
193. Lemaitre J (ed.) (2001) *Continuous damage*. In: *Handbook of Materials Behavior Models*, Academic Press, San Diego, CA, 411–793

194. Leppin C, Li J, Daniel D (2008) Application of a method to correct the effect of non-proportional strain paths on Nakajima test based Forming Limit Curves. In: Hora P (ed) Proc. of the NUMISHEET 2008 Conf., Interlaken, Switzerland, 217–221
195. Lewison DJ, Lee D (1999) Determination of forming limits by digital image processing methods. In: Proceedings of International Body Engineering Conference and Exposition (IBEC), Detroit (MI), (Paper 01-3168)
196. Li S, Hoferlin E, Van Bael A, Van Houtte P (2001) Application of a texture-based plastic potential in earing prediction of an IF steel. *Adv. Eng. Materials*, 990–994
197. Liebertz H, et al. (2004) Guideline for the determination of forming limit curves. In: Proc. of the IDDRG Conference, Sindelfilgen, 216–224
198. Lin SB, Ding JL (1995) Experimental study of the plastic yielding of rolled sheet metals with the cruciform plate specimen. *Int J Plast* 11:583–604
199. Liu C, Huang Y, Stout MG (1997) On the asymmetric yield surface of plastically orthotropic materials: a phenomenological study. *Acta Mater* 45:2397–2406
200. Logan RW, Hosford WF (1980) Upper-bound anisotropic yield locus calculations assuming pencil glide. *Int J Mech Sci* 22:419–430
201. Lou XY, Li M, Boger RK, Agnew SR, Wagoner RH (2007) Hardening evolution of AZ31B Mg sheet. *Int J Plast* 23:44–86
202. Lowden MAW, Hutchinson WB (1975) Texture strengthening and strength differential in titanium-6A-4V. *Metall Trans* 6A:441–448
203. Makinde A, Thibodeau L, Neale KW (1992) Development of an apparatus for biaxial testing using cruciform specimens. *Exp Mech* 32:138–144
204. Maeda Y, Yanagawa M, Barlat F, Chung K, Hayashida Y, Hattori S, Matsui K, Brem JC, Lege DJ, Murtha SJ, Ishikawa T (1998) Experimental analysis of aluminum yield surface for binary Al-Mg alloy sheet samples. *Int J Plast* 14:301–318
205. Marciniak Z, Kuczynski K (1967) Limit strains in the processes of stretch forming sheet metal. *Int J Mech Sci* 9:609–620
206. Marron G, et al. (1997) A new necking criterion for the forming limit diagrams, IDDRG 1997 WG Meeting, Haugesund
207. Martin PH, Smith LM (2005) Practical limitations to the influence of through-thickness normal stress on sheet metal formability. *Int J Plast* 21:671–690
208. Mattiasson K, Sigvant M, Larsson M (2007) On the prediction of plastic instability in metal sheets, In: César de Sá JMA, Santos, AD (eds) Proc. NUMIFORM'07 Conference 908, 129–135
209. Mattiasson K, Sigvant M, Larsson M (2007) Theoretical and experimental sheet metal failure evaluation. In: Tisza M (ed) Proc. of the IDDRG 2007 Conference, Gyor, 185–194
210. Mattiasson K, Sigvant M, Larsson M (2008) On the role of strain rate in finite element simulations of sheet forming processes. In: Hora P (ed) Proc. of the NUMISHEET 2008 Conf. (Part B. Benchmark study), Interlaken, Switzerland, 223–228
211. Mattiasson K, Sigvant M (2008) An evaluation of some recent yield criteria for industrial simulations of sheet forming processes. *Int J Mech Sci* 50:774–787
212. McDowell DL (2000) Modeling and experiments in plasticity. *Int J Solids Struct* 37:293–309
213. McGinty R, McDowell DL (2004) Application of multiscale crystal plasticity models to FLD. *TransASME, J Eng Mater Techn* 126:285–291
214. Mellor PB (1981) Sheet metal forming. *Int Met Rev* 1:1–20
215. Mellor PB, Parmar A (1978) Plasticity analysis of sheet metal forming. In: Koistinen DP, Wang NM (eds) *Mechanics of sheet metal forming*. Plenum, New York, pp 53–74
216. Methods of determining the forming limit curve. IDDRG Meeting, Zurich (1983)
217. Michno MJ Jr, Findley WN (1976) An historical perspective of yield surface investigations for metals. *Int J Non Lin Mech* 11:59–82
218. Miyauchi K (1984) Bauschinger effect in planar shear deformation of sheet metals. In: *Advanced Technology of Plasticity*, Proc. 1st Int. Conf. Technology of Plasticity, The Japan Society for Technology of Plasticity, Tokyo, 623
219. Mohr D, Oswald M (2008) A new experimental technique for the multi-axial testing of advanced high strength steel sheets. *Exp Mech* 48:65–77
220. Moondra S, Kinsey BL (2004) Determination of cruciform specimen for stress based failure criterion evaluation. *Trans. NAMRI/SME*, 247–254.
221. Müller W, Pöhlandt KJ (1996) New experiments for determining yield loci of sheet metal. *J Mater Process Tech* 60:643–648
222. Naka T, Nakayama Y, Uemori T, Hino R, Yoshida F (2004) Effect of strain-rate and temperature on yield locus for 5083 aluminum alloy sheet. *Key Engineering Materials* 274–276:937–942
223. Nakazima K, Kikuma T, Hasuka K (1971) Study on the formability of steel sheets. *Yawata Tech Rep No 284:678–680*
224. Nandedkar VM, Narashimhan K (1999) Prediction of forming limits incorporating work-hardening behavior. In: Gelin JC, Picart P (eds) Proc. of the NUMISHEET 1999 Conference, Besancon, 437–442
225. Narashimhan K, Wagoner RH (1991) Finite element modeling simulation of in-plane FLD of sheets containing finite defects. *Metall Trans* 22A:2655–2665
226. Nixon ME, Cazacu O, Lebensohn RA (2010) Anisotropic response of high-purity α -titanium: Experimental characterization and constitutive modeling. *Int J Plast* 26:510–532
227. Paraianu L, Banabic D (2005) Calculation of forming limit diagrams using a finite element model. In: Banabic D (ed) Proc. 8th ESAFORM Conference on Material Forming. Cluj-Napoca, April 2005. The Publishing House of the Romanian Academy, Bucharest, 419–423
228. Paraianu L, Comsa DS, Gracio JJ, Banabic D (2006) Influence of yield locus and strain-rate sensitivity on the Forming Limit Diagrams. In: Juster N, Rosochowski A (eds) Proc. 9th ESAFORM Conference on Material Forming, Glasgow, April 2006, The Publishing House AKAPIT, Krakow, 343–346
229. Parsa MH, Etehad M, Nasher AI Ahkami S (2009) FLD determination of Al 3105/polypropylene/Al 3105 sandwich sheet using numerical calculation and experimental investigations. In: van den Boogart T, Akkerman R (eds) Proc. of the 12th ESAFORM Conference on Material Forming, Enshede
230. Petek A, Kuzman K (2007) The determination of the FLD for conventional and single point incremental sheet metal forming. In: Tisza M (ed) Proc. of the IDDRG 2007 Conference, Gyor, 249–256
231. Phillips A (1986) A review of quasistatic experimental plasticity and viscoplasticity. *Int J Plast* 2:315–328
232. Plunkett B, Lebensohn RA, Cazacu O, Barlat F (2006) Anisotropic yield function of hexagonal materials taking into account texture development and anisotropic hardening. *Acta Mater* 54:4159–4169
233. Plunkett B, Cazacu O, Barlat F (2008) Orthotropic yield criteria for description of the anisotropy in tension and compression of sheet metals. *Int J Plast* 24:847–866
234. Plunkett B, Cazacu O (2008) Viscoplastic modeling of anisotropic textured metals. In: *Multiscale modeling of heterogeneous materials: from microstructure to macroscale properties*. In: Cazacu O (ed) ISTE Ltd and John Wiley & Sons, Inc, 71–91
235. Plunkett B, Cazacu O, Lebensohn RA, Barlat F (2008) Elastic-viscoplastic anisotropic constitutive modeling of textured metals and validation using the Taylor cylinder impact test. *Int. J. Plast*, 1001–1021.

236. Rabahallah M, Balan T, Bouvier S, Bacroix B, Barlat F, Chung K, Teodosiu C (2009) Parameter identification of advanced plastic strain rate potentials and impact on plastic anisotropy prediction. *Int J Plast* 25:491–512
237. Rabahallah M, Balan T, Bouvier S, Teodosiu C (2009) Time-integration for elasto-plastic models based on anisotropic strain rate potentials. *Int J Numer Meth Eng* 80:381–402
238. Rajarajan G, et al. (2005) Validation of the non-linear strain–path model CRACH to enhance the interpretation of FE simulations in multistage forming operations, In: Banabic D (ed) Proc. 8th ESAFORM Conference on Material Forming. Cluj-Napoca, April 2005. The Publishing House of the Romanian Academy, Bucharest, 387–390
239. Ragab AR, Saleh C (2000) Effect of void growth on the predicting forming limit strains for planar isotropic sheet metals. *Mech Mater* 32:71–84
240. Ragab AR, Saleh C, Zafarani NN (2002) Forming limit diagrams for kinematically hardened voided sheet metals. *J Mater Process Tech* 128:302–312
241. Ranta-Eskola AJ (1979) Use of the hydraulic bulge test in biaxial tensile testing. *Int J Mech Sci* 21:457–465
242. Rechberger F, Till ET (2004) Influence of scatter of materials properties on the formability of parts. In: Kergen R (ed) Forming the future, Proc. IDDRG 2004 Conference, Sindelfingen, 236–245
243. Savoie J et al (1998) Prediction of the FLD using crystal plasticity model. *Mater Sci Eng A* 257:128–133
244. Shakeri M, Sadough A, Dariani BM (2000) Effect of pre-straining and grain size on the limit strains in sheet metal forming. *Proc Inst Mech Eng* 214B:821–827
245. Schatz M, Keller S, Feldmann P (2005) Experimental determination of the FLD for sheet thickness from 2.5 to 5.0 mm (in German). *UTF Science III*, 1–8
246. Shim MS, Park JJ (2001) The formability of aluminium sheet in incremental forming. *J Mater Process Tech* 113:654–658
247. Signorelli JW, Bertinetti MA, Turner PA (2009) Predictions of forming limit diagrams using a rate-dependent polycrystal self-consistent plasticity model. *Int J Plast* 25:1–25
248. Signorelli JW, Bertinetti MA (2009) On the role of constitutive model in the forming limit of FCC sheet metal with cube orientations. *Int J Mech Sci* 51:473–480
249. Simha CHM, Gholipour J, Bardelcik A, Worswick MJ (2007) Prediction of necking in tubular hydroforming using an extended stress-based FLC. *ASME J Eng Mater Technol* 129:136–47
250. Simha CHM, Grantab R, Worswick MJ (2007) Computational analysis of stress-based forming limit curves. *Int J Solids Struct* 44:8663–8684
251. Shiratori E, Ikegami K (1968) Experimental study of the subsequent yield surface by using cross-shaped specimens. *J Mech Phys Solid* 16:373–394
252. Smith LM et al (2003) Influence of transverse normal stress on sheet metal formability. *Int J Plast* 19:1567–1583
253. Soare S, Yoon J., Cazacu O (2007) On using homogeneous polynomials to design anisotropic yield functions with tension/compression symmetry/asymmetry. In: Cesar de Sa, JMA, Santos AD (eds) Materials processing and design: modeling, simulation and Applications. Proc. of the NUMIFORM 2007 Conf., Porto, 607–612
254. Soare S, Banabic D (2008) Application of a polynomial yield function to the predictions of limit strains. *Steel Res Int* 79:39–46
255. Soare S, Banabic D (2009) A discussion upon the sensitivity of the MK model to input data. *Int. Journal Material Forming*, 2, (doi:10.1007/s12289-008-0347-y)
256. Spitzig WA, Richmond O (1984) The effect of pressure on the flow stress of metals. *Acta Metall* 32:457–463
257. Stout MG, Kocks UF (1998) Effects of Texture on Plasticity. In: Kocks UF, Tomé CN, Wenk H-R (eds) *Texture and anisotropy*. Cambridge University Press, Cambridge, pp 420–465
258. Stoughton TB (2000) A general forming limit criterion for sheet metal forming. *Int J Mech Sci* 42:1–27
259. Stoughton TB, Zhu X (2004) Review of theoretical models of the strain-based FLD and their relevance to the stress-based FLD. *Int J Plast* 20:1463–1486
260. Stoughton TB, Yoon JW (2005) Sheet metal formability analysis for anisotropic materials under non-proportional loading. *Int J Mech Sci* 47:1972–2002
261. Stoughton TB (2008) Generalized metal failure criterion. In: Hora P (ed) Proc. of the NUMISHEET 2008 Conf. (Part B. Benchmark study), Interlaken, Switzerland, 241–246
262. Stören S, Rice JR (1975) Localized necking in thin sheets. *J Mech Phys Solid* 23:421–441
263. Strano M, Colosimo BM (2006) Logistic regression analysis for experimental determination of forming limit diagrams. *Int J Mach Tool Manufact* 46:673–682
264. Strano M, Colosimo BM (2006) Ordinal logistic regression analysis for statistical determination of forming limit diagrams. In: Juster N, Rosochowski A (eds) Proc. 9th ESAFORM Conference on Material Forming, Glasgow, April 2006, The Publishing House AKAPIT, Krakow, 303–306
265. Swift HW (1952) Plastic instability under plane stress. *J Mech Phys Sol* 1:1–16
266. Szczepiński W (ed) (1990) *Experimental methods in mechanics of solids*. Elsevier, Amsterdam
267. Tai WH, Lee WB (1996) Finite element simulation of in plane forming processes of sheets containing plastic damage. In: Lee JK, Kinzel GL, Wagoner RH (eds) Proc. of the NUMISHEET 1996 Conference, Dearborn, 257–261
268. Takashina K et al (1968) Relation between the manufacturing conditions and the average strain according to the scribed circle tests in steel sheets. *La Metallurgia Italiana* 8:757–765
269. Teixeira P, et al. (2006) Finite element prediction of fracture onset in sheet metal forming using a ductile damage model. In: Proc. of the IDDRG 2006 Conference, Porto, 239–245
270. Teodosiu C, Hu H (1995) Microstructure in the continuum modeling of plastic anisotropy. In: Shen S, Dawson PR (eds) Proc. of the Conference, NUMIFORM’95 on Simulation of Materials Processing, Theory, Methods and Applications, Balkema, Rotterdam, 173
271. Thoors H, et al. (2008) FLD assessment using the proposed new standard. IDDRG 2008 International Conference, Olofström, Sweden, 25–35
272. Tozawa Y (1978) Plastic deformation behavior under conditions of combined stress. In: Koistinen DP, Wang N-M (eds) *Mechanics of sheet metal forming*. Plenum, New York, pp 81–110
273. Van der Boogaard AH, Huetink J (2003) Prediction of sheet necking with shell finite element models. In: Brucato V (ed) Proc. 6th ESAFORM Conference on Material Forming, Salerno, April 2003, Nuova Ipsa Editore, Palermo, 191–194
274. Van Bael A, Van Houtte P (2002) Convex fourth and sixth-order plastic potentials derived from crystallographic texture. In: Cescotto S (ed) Proceedings of the 6th European Mechanics of Materials Conference (EMMC6), University of Liege, Liege, Belgium, 51–58
275. Van Houtte P, Toth LS (1993) Generalization of the Marciniak-Kuczynski defect model for predicting FLD. In: Lee WB (ed) *Advances in engineering plasticity and its application*. Elsevier, Amsterdam, pp 1013–1020
276. Van Houtte P (1994) Application of plastic potentials to strain rate sensitive and insensitive anisotropic materials. *Int J Plast* 10:719–748

277. Van Houtte P (2001) Yield loci based on crystallographic texture. In: Lemaitre J (ed) Handbook of materials behavior models. Academic, San Diego, pp 137–154
278. Van Houtte P (2005) Anisotropy and formability in sheet metal drawing. In: Banabic D (ed) Proc. 8th ESAFORM Conference on Material Forming. Cluj-Napoca, April 2005. The Publishing House of the Romanian Academy, Bucharest, 339–342
279. Van Minh H, Sowerby R, Duncan JL (1973) Variability of forming limit curves. *Int J Mech Sci* 16:31–44
280. Van Riel M, Van den Boogaard AH (2008) A strain path change indicator for use in sheet metal forming processes. *Proc IDDRG 2008*:279–290
281. Veerman C, et al. (1971) Determination of appearing and admissible strains in cold-reduced sheets. *Sheet Metal Industries*, 687–694
282. Vegter H, An Y, Pijlman HH, Huetink J (1999) Different approaches to describe the plastic material behaviour of steel and aluminium-alloys in sheet forming. In: Covas JA (ed) Proc. of the 2nd ESAFORM Conference on Material Forming. Guimaraes, 127–132
283. Vegter H, van den Boogaard AH (2006) A plane stress yield function for anisotropic sheet material by interpolation of biaxial stress states. *Int J Plast* 22:557–580
284. Vegter H, ten Horn CHLJ, Abspoel M (2008) Modeling of the Forming Limit Curve by MK Analysis and FE simulations. In: Hora P (ed) Proc. of the NUMISHEET 2008 Conf. (Part B. Benchmark study), Interlaken, Switzerland, 187–192
285. Viatkina, E.M. et al.: Forming Limit Diagrams for sheet deformation process: a crystal plasticity approach. In: Habraken AM (ed) Proc. of the 4th ESAFORM Conference on Material Forming, Liege (2001) 465–468.
286. Vitek V, Mrovec M, Bassani JL (2004) Influence of non-glide stresses on plastic flow: from atomistic to continuum modeling. *Mater Sci Eng A* 365:31–37
287. Volk W (2006) New experimental and numerical approach in the evaluation of the FLD with the FE-method. In: Hora P (ed) Numerical and experimental methods in prediction of forming limits in sheet forming and tube hydroforming processes. ETH, Zürich, pp 26–30
288. Volk W, et al. (2008) Benchmark 1 virtual forming limit curves. Part A. Physical tryout report. In: Hora P (ed) Proc. of the NUMISHEET 2008 Conf. (Part B. Benchmark study), Interlaken, Switzerland, 3–9
289. Volk W, et al. (2008) Benchmark 1 virtual forming limit curves. Part B. Benchmark analysis. In: Hora P (ed) Proc. of the NUMISHEET 2008 Conf. (Part B. Benchmark study), Interlaken, Switzerland, 11–42
290. Vos M, Banabic D (2007) The forming limit band—a new tool for increasing the robustness in the simulation of sheet metal forming processes. Proc. of the IDDRG 2007 Conference, Gyor, 165–176
291. Wagoner RH, Chan KS, Keeler SP (eds) (1989) Forming limit diagrams: concepts, methods, and applications. TMS, Warrendale
292. Weinmann KJ, Rosenberger AH, Sanchez LR (1988) The Bauschinger effect of sheet metal under cyclic reverse pure bending. *Ann CIRP* 37:289–293
293. Wu PD, Neale KW, Van der Giessen E (1997) On crystal plasticity FLD analysis. *Proc R Soc Lond* 453:1831–1848
294. Wu PD et al (1998) Crystal plasticity FLD analysis of rolled aluminium sheets. *Metall Trans* 29A:527–535
295. Wu PD, MacEwen SR, Lloyd DJ, Neale KW (2004) A mesoscopic approach for predicting sheet metal formability. *Model Simulat Mater Sci Eng* 12:511–527
296. Wu PD, Graf A, MacEwen SR, Lloyd DJ, Jain M, Neale KW (2005) On forming limit stress diagram analysis. *Int J Solids Struct* 42:2225–2241
297. Wu PD, Lloyd DJ, Jain M, Neale KW, Huang Y (2007) Effects of spatial grain orientation distribution and initial surface topography on sheet metal necking. *Int J Plast* 23:1084–1104
298. Wu PD et al (2008) Effects of superimposed hydrostatic pressure on sheet metal formability. *Int J Plast* 25:1711–1725
299. Xu Y (2006) Modern formability: measurement, analysis and applications. Hanser Gardner Publications
300. Yao H, Cao J (2002) Prediction of FLC using an anisotropic yield function with prestrain induced prestress. *Int J Plast* 18:1013–1038
301. Young RF, Bird JE, Duncan JL (1981) An automated hydraulic bulge tester. *J Appl Metalwork* 2:11–18
302. Yoon JW, Song IS, Yang DY, Chung K, Barlat F (1995) Finite element method for sheet forming based on an anisotropic strain-rate potential and the convected coordinate system. *Int J Mech Sci* 37(1995):733–752
303. Yoon JW, Barlat F, Dick RE, Chung K, Kang TJ (2004) Plane stress yield function for aluminum alloy sheets—Part II: FE formulation and its implementation. *Int J Plast* 20:495–522
304. Yoon JW, Barlat F, Dick RE, Karabin ME (2006) Prediction of six or eight ears in a drawn cup based on a new anisotropic yield function. *Int J Plast* 22:174–193
305. Yoon JW, Barlat F (2006) Modeling and simulation of the forming of aluminium sheet alloys. In: Semiatin SL (ed) ASM handbook, Vol 14B, Metalworking: sheet forming. ASM International, Materials Park, pp 792–826
306. Yoshida F, Urabe M, Toropov VV (1998) Identification of material parameters in constitutive model for sheet metals from cyclic bending tests. *Int J Mech Sci* 40:237–249
307. Yoshida F, Uemori T, Fujiwara K (2002) Elastic–plastic behavior of steel sheets under in-plane cyclic tension–compression at large strain. *Int J Plast* 18:633–659
308. Yoshida K, Kuwabara T, Narihara K, Takahashi S (2005) Experimental verification of the path-independence of forming limit stresses. *Int J Form Process* 8(SI):283–298
309. Yoshida K, Kuwabara T, Kuroda M (2007) Path-dependence of the forming limit stresses in a sheet metal. *Int J Plast* 23:361–384
310. Yoshida K, Kuwabara T (2007) Effect of strain hardening behavior on forming limit stresses of steel tube subjected to non-proportional loading paths. *Int J Plast* 23:1260–1284
311. Yu MH (2002) Advances in strength theories for materials under complex stress state in the 20th Century. *Appl Mech Rev* 55:198–218
312. Yu Y, Wan M, Wu X-D, Zhou X-B (2002) Design of a cruciform biaxial tensile specimen for limit strain analysis by FEM. *J Mater Process Tech* 123:67–70
313. Zhang C, et al. (2008) Theoretical and numerical study of strain rate sensitivity on formability of sheet metal. In: Hora P (ed) Proc. of the NUMISHEET 2008 Conf., Interlaken, Switzerland, 229–233
314. Zhou D, Wagoner RH (1991) Use of arbitrary yield function in FEM. In: Boehler JP, Khan AS (eds) Anisotropy and localization of plastic deformation. Elsevier, Amsterdam, pp 688–691
315. Zhou Y, Neale KW (1995) Predictions of FLD using a rate sensitive crystal plasticity model. *Int J Mech Sci* 37:1–20
316. Ziegler H (1977) An introduction to thermodynamics. North-Holland, Amsterdam
317. Źyczkowski M (1981) Combined loadings in the theory of plasticity. Polish Scientific, Warsaw
318. Źyczkowski M (2001) Anisotropic yield condition. In: Lemaitre J (ed) Handbook of materials behaviour models. Academic, San Diego, pp 155–165